JPET Fast Forward. Published on February 4, 2015 as DOI: 10.1124/jpet.114.221242
This article has not been copyedited and formatted. The final version may differ from this version.

Title Page.

Anti-PCSK9 Antibody Pharmacokinetics and LDL-C Pharmacodynamics in Non-Human Primates Are Antigen Affinity-Dependent and Exhibit Limited Sensitivity to FcRn Binding Enhancement

Kirk R. Henne, Brandon Ason, Monique Howard, Wei Wang, Jeonghoon Sun, Jared Higbee, Jie Tang, Katherine C. Matsuda, Ren Xu, Lei Zhou, Joyce C. Y. Chan, Chadwick King, Derek E. Piper, Randal R. Ketchem, Mark Leo Michaels, Simon M. Jackson, and Marc W. Retter.

Departments of Pharmacokinetics and Drug Metabolism (KRH, KCM, MWR), Metabolic Disorders (BA, JCYC, SMJ), Therapeutic Discovery (MH, WW, JS, JH, JT, CK, DEP, RRK, MLM), Molecular Sciences (RX), and Biostatistics (LZ), Amgen, Inc., South San Francisco, California

JPET Fast Forward. Published on February 4, 2015 as DOI: 10.1124/jpet.114.221242
This article has not been copyedited and formatted. The final version may differ from this version.

Running Title Page.

Running Title: "PCSK9 and FcRn Binding Affinities Affect Antibody PK and PD"

Address for Correspondence:

Kirk R. Henne

Amgen, Inc.

1120 Veterans Boulevard

South San Francisco, CA 94080

Ph: 650-244-2154

Fax: 650-871-2934

Email: khenne@amgen.com

Text pages: 42

Tables: 4 (+ 6 Supplemental)

Figures: 4 (+ 1 Supplemental)

References: 42

Abstract words: 243

Introduction words: 793

Discussion words: 1637

Abbreviations: PCSK9, proprotein convertase subtilisin/kexin type 9; LDL-C, low density lipoprotein-cholesterol; LDLR, low density lipoprotein receptor; PK, pharmacokinetic(s); NCA, non-compartmental analysis; PD, pharmacodynamic(s); ECA, effect curve area; TMD, target-mediated disposition, mAb, monoclonal antibody; Fab, fragment, antigen-binding; Fc, fragment, crystallizable; CDR, complementarity determining region; FcRn, neonatal Fc receptor; SPR, surface plasmon resonance.

JPET Fast Forward. Published on February 4, 2015 as DOI: 10.1124/jpet.114.221242
This article has not been copyedited and formatted. The final version may differ from this version.

Recommended Section Assignment: Drug Discovery and Translational Medicine

Abstract.

Proprotein convertase subtilisin/kexin type 9 (PCSK9) has emerged as an attractive therapeutic target for cardiovascular disease. Monoclonal antibodies (mAbs) that bind PCSK9 and prevent PCSK9:LDLR complex formation reduce serum LDL-C in vivo. PCSK9-mediated lysosomal degradation of bound mAb, however, dramatically reduces mAb exposure and limits duration of effect. Administration of high affinity mAb1:PCSK9 complex (1:2) to mice resulted in significantly lower mAb1 exposure compared to mAb1 dosed alone in normal mice or in PCSK9 knock-out mice lacking antigen. To identify mAb binding characteristics that minimize lysosomal disposition, the pharmacokinetic behavior of four mAbs representing a diverse range of PCSK9 binding affinities at neutral (serum) and acidic (endosomal) pH was evaluated in cynomolgus monkeys. Results revealed an inverse correlation between affinity and both mAb exposure and duration of LDL-C lowering. High affinity mAb1 exhibited the lowest exposure and shortest duration of action (6 days), while mAb2 displayed prolonged exposure and LDL-C reduction (51 days) as a consequence of lower affinity and pH-sensitive PCSK9 binding. mAbs with shorter endosomal PCSK9:mAb complex dissociation half-lives (<20 seconds) produced optimal exposure-response profiles. Interestingly, incorporation of previously reported Fc-region amino acid substitutions or novel “loop-insertion” peptides that enhance in vitro FcRn binding led to only modest PK improvements for mAbs with pH-dependent PCSK9 binding, with only limited augmentation of PD activity relative to native mAbs. A pivotal role for PCSK9 in mAb clearance was demonstrated, more broadly suggesting that therapeutic mAb binding characteristics require optimization based on target pharmacology.

JPET Fast Forward. Published on February 4, 2015 as DOI: 10.1124/jpet.114.221242
This article has not been copyedited and formatted. The final version may differ from this version.

Introduction.

Morbidity and mortality rates remain high in patients with cardiovascular disease (CVD) despite the utility of widely prescribed statin medications, which up-regulate expression of low density lipoprotein receptor (LDLR) in the liver and reduce circulating cholesterol containing low density lipoprotein (LDL-C) (Grundy et al., 2004; Stancu and Sima, 2001), an established risk factor for the disease. Since aggressive plasma LDL-C lowering is associated with reduced risk for CVD (Cholesterol Treatment Trialists et al., 2010), novel therapies resulting in even lower LDL-C may further reduce disease risk.

Proprotein convertase subtilisin/kexin type 9 (PCSK9), a serine protease consisting of a prodomain, catalytic domain, and C-terminal cysteine-histidine rich domain (Piper et al., 2007), has been implicated as an important regulator of LDL-C (Horton et al., 2007). PCSK9 protein is expressed primarily in the liver and secreted into circulation (Seidah et al., 2003) where it binds LDLR on the liver cell surface. The resulting LDLR:PCSK9 complex enters the cell and is transported to the lysosome compartment and degraded (Lagace et al., 2006). In contrast, internalized LDLR:LDL-C complex dissociates within the endosome allowing for LDLR transport back to the cell surface while LDL-C is processed in the lysosome (Brown et al., 1997). Human subjects with PCSK9 gain-of-function and loss-of-function mutations have higher and lower circulating LDL-C, and higher and lower CVD risk, respectively, than subjects with wild-type PCSK9 (Abifadel et al., 2003; Cohen et al., 2006).

PCSK9-specific monoclonal antibodies (mAbs) have been generated that inhibit interaction between PCSK9 and LDLR, preventing PCSK9-mediated LDLR degradation in preclinical species (Chan et al., 2009; Liang et al., 2012; Ni et al., 2011). These neutralizing mAbs increase hepatocyte LDLR levels and concomitantly increase hepatic LDL-C clearance, serving to reduce plasma LDL-C levels. Inhibition of PCSK9 function by mAb intervention or other

JPET Fast Forward. Published on February 4, 2015 as DOI: 10.1124/jpet.114.221242
This article has not been copyedited and formatted. The final version may differ from this version.

modality, such as adnectins or siRNA, has also resulted in LDL-C reduction in human subjects (Hooper and Burnett, 2013; Stein and Raal, 2014). Clinically, anti-PCSK9 mAbs have shown promise as monotherapy, in combination with other treatments like statins (Robinson et al., 2014) which are known to increase PCSK9 expression (Careskey et al., 2008), or as treatment in statin intolerant populations (Stroes et al., 2014).

Like LDLR, anti-PCSK9 mAbs are hypothesized to undergo lysosomal degradation when bound to PCSK9, and are therefore subjected to target-mediated disposition (TMD). As a consequence of TMD, PK properties of therapeutics can be negatively impacted (Levy, 1994), often leading to the requirement for higher doses or more frequent administration to maintain PD effect. Dose-dependent PK, a hallmark of TMD, has recently been described for a "high" affinity (K_D=0.120 nM) anti-PCSK9 mAb (Chaparro-Riggers et al., 2012). The mechanism of PCSK9-mediated degradation of LDLR or bound antibody is not fully understood, but other PCSK9 interacting proteins such as amyloid precursor-like protein 2 (APLP2) have been implicated (DeVay et al., 2013).

Attempts to minimize TMD impact have focused on engineering mAb antigen-binding properties to promote pH-dependent release of antigen in acidified endosomes. This approach has been successfully applied to a mAb recognizing IL-6 receptor (a cell membrane-associated target) and PCSK9 (a soluble protein ligand), where improvements in non-human primate PK and PD were observed (Chaparro-Riggers et al., 2012; Igawa et al., 2010). Modulation of pH-dependent interactions with neonatal Fc receptor, FcRn (Roopenian and Akilesh, 2007), may also help minimize TMD impact. IgG-FcRn interactions are pH-dependent, characterized by high affinity binding at pH 5.5 in the endosome to promote recycling by protecting mAbs from catabolism, followed by extracellular release at pH 7.4 as a result of reduced affinity. Numerous examples have been described where IgG Fc-region amino acid substitutions enhance pH-dependent FcRn binding, leading to improved PK properties in preclinical species (Dall'Acqua et

al., 2006; Dall'Acqua et al., 2002; Finch et al., 2011; Hinton et al., 2004; Zalevsky et al., 2010) or humans (Robbie et al., 2013). An effort combining both pH-dependent antigen affinity optimization with enhanced FcRn binding has been reported for tocilizumab (Igawa et al., 2010).

This current work describes an endeavor to identify kinetic aspects of pH-dependent PCSK9 binding that are most crucial for retaining desired mAb PK properties and eliciting optimal PD outcomes. Results from the characterization of a panel of four PCSK9-specific mAbs are presented, wherein affinity for PCSK9 and degree of pH-sensitive binding varied across the panel. mAb PK attributes and LDL-C reduction in non-human primates served as primary endpoints for evaluation. Combination of pH-sensitive antigen binding with improved FcRn binding was also assessed. Selected mAbs containing previously described Fc-region amino acid substitutions “YTE” (Dall'Acqua et al., 2002) or “LS” (Zalevsky et al., 2010) were studied alongside two novel peptide Fc “loop-insertion” variants with improved in vitro FcRn affinity. Overall, antibody engineering to optimize pH-dependent PCSK9 binding was demonstrated to have a more significant impact on anti-PCSK9 mAb PK and PD than enhanced FcRn binding.

Materials and Methods.

Anti-PCSK9 Monoclonal Antibody Generation and Characterization. The fully-human monoclonal antibody, mAb1, was generated as previously described (Chan et al., 2009). In brief, mice engineered to express human IgG antibodies were immunized with recombinant human PCSK9 antigen (Amgen, Inc.). Hybridomas were generated and the resulting monoclonal antibodies were evaluated for PCSK9 binding and inhibition of the PCSK9:LDLR interaction. Characterization of human PCSK9 binding affinity, cross-reactivity to mouse and cynomolgus monkey PCSK9, and activity in a cell-based LDL uptake assay led to identification of multiple antibodies, from which mAb1 was selected.

Antibody mAb2 was identified in a subsequent screen of the aforementioned hybridoma mAbs (ranked initially by inhibition of the PCSK9:LDLR interaction), where pH-dependent binding to human PCSK9 was added as a selection criterion. Biotin-labeled human PCSK9 was attached to neutravidin-coated 384-well plates, and spent hybridoma supernatant was diluted and added to the wells. The pH was adjusted to either 7.4 or 6.0, and the plate was incubated at room temperature for 2 h. Antibody binding to PCSK9 was measured by ELISA using a peroxidase-labeled anti-human IgG Fc antibody. mAb2 exhibited greater binding at pH 7.4 relative to 6.0 by a factor of ~2 under the conditions of the assay.

Additional efforts to generate anti-PCSK9 antibodies with specific PCSK9 binding properties included an analysis of a mAb2:PCSK9 co-crystal structure to identify CDR-derived amino acid residues within 6 Å of PCSK9. A total of 34 residues met this criterion. Using a computational genetic algorithm for protein design (Pokala and Handel, 2005), PCSK9 binding free energy (bound–unbound) was determined for native mAb2 to arrive at a baseline ΔG for ligand binding. Amino acid substitutions at each of the 34 identified positions were subsequently modeled in order to determine their effect on binding free energy (mutated–parental), giving rise to a series

of ΔΔG values. Calculations were performed for more than 140,000 unique amino acid combinations to identify those that lowered the bound energy state. A panel of 168 of the lowest ΔΔG variant-containing mAbs was cloned, expressed, and tested for cynomolgus monkey PCSK9 binding affinity at pH 7.4 and 5.5 by surface plasmon resonance (SPR) analysis. Both mAb3 and mAb4 were identified as a result of this screen.

All the selected antibodies, mAb1, mAb2, mAb3, and mAb4, were of the IgG2 subclass. The IgG2 Control mAb utilized for in vivo mouse and cynomolgus monkey PK/PD experiments was a human anti-keyhole limpet hemocyanin (KLH) monoclonal antibody (Amgen, Inc.).

Antibody:PCSK9 Complex Formation and Isolation. High-affinity anti-PCSK9 antibodies formed mono- and bivalent antigen complexes that were sufficiently stable to allow for analytical purification. mAb1 and recombinant human PCSK9 were diluted into 1xPBS to final concentrations of 0.4 mg/mL and 0.7 mg/mL, respectively, and incubated at 4°C for 2 h. Bivalent mAb1:huPCSK9 complex was isolated by resolving gel filtration using an ÄKTAexplorer 100 Air workstation (GE Healthcare Bio-Sciences, Pittsburgh, PA) coupled to a 2.6x60 cm HiLoad™ 26/600 Superdex™ 200 prep grade column (GE Healthcare Bio-Sciences). Eluent was 1xPBS eluent at a 3 mL/min flow rate. Eluted fractions exhibiting the expected bivalent complex molecular weight were pooled, and protein concentration was determined by A280 absorbance on a SpecraMax M2e microplate reader (Molecular Devices, Sunnyvale, CA). Polydispersity was assessed by dynamic light scattering (DLS). Analyses were performed in triplicate with multiple 4–10 s acquisitions on a DynaPro® Plate Reader II (Wyatt Technology, Santa Barbara, CA). The mAb1:PCSK9 complex molecular weight was estimated using hydrodynamic radius values calculated from the Stokes-Einstein equation. A molecular weight estimate of 388 kDa confirmed binding stoichiometry of 1:2 in the resolved complex (similar analyses for mAb1 and human PCSK9 yielded molecular weight estimates of 205 and 87 kDa, respectively).

Antibody Fab:PCSK9 Binding Affinity Characterization. Generation of Fabs from mAb1–4 was performed using a Pierce Fab preparation kit (Thermo Scientific, Waltham, MA). Kinetic rate coefficients for mAb1, mAb2, mAb3, and mAb4 Fab binding to recombinant cynomolgus monkey PCSK9 (Amgen, Inc.) at pH 7.4 or 5.5 were recovered from SPR binding experiments performed with a ProteOn™ XPR36 Protein Interaction Array System using an NLC sensor chip (Bio-Rad Laboratories, Inc., Hercules, CA). Analytes were injected at 25º C over multiple PCSK9-biotin captured surfaces at concentrations of 0.137–33.3 nM (pH 7.4) or 0.137–900 nM (pH 5.5). The association phase was collected for 480 s, and the dissociation phase was collected until the data returned to baseline (with a maximum of 7200 s). Data were aligned and double-referenced using ProteOn Manager©, v3.1.06 (Bio-Rad Laboratories, Inc.), and were then fit to a 1:1 binding model using Scrubber© software, v2.0 (BioLogic Software Pty Ltd, Campbell, Australia). The dissociation phase was fit globally to a first-order exponential decay equation to recover the respective dissociation rate coefficients, which were subsequently used as fixed parameters in the global analyses of the respective association phase data. R_{max} values were grouped for each PCSK9 surface. Complex dissociation half-lives at pH 5.5 were determined using k_d values derived from the kinetic analyses ($\ln 2/k_d$).

Anti-PCSK9 mAb Fc-Region Modifications for Enhanced FcRn Binding. IgG Fc-region amino acid substitutions M252Y/S254T/T256E, designated YTE (Dall'Acqua et al., 2002), and M428L/N434S, designated LS (Zalevsky et al., 2010), were previously shown to enhance FcRn binding affinity of IgG in vitro and improve PK properties of mAbs in non-human primates (Dall'Acqua et al., 2006; Zalevsky et al., 2010). These mutations were introduced into the IgG2 heavy chains of mAb1 and mAb2 by site-directed mutagenesis using a QuikChange kit (Agilent Technologies, Inc., Santa Clara, CA). Plasmids containing heavy chain or light chain cassettes were co-transfected into Chinese hamster ovary (CHO) cells for stable expression. Expressed antibodies were purified by chromatography using MabSelect SuRe followed by SP-Sepharose

(GE Healthcare Bio-Sciences) as previously described (Chan et al., 2009). Purified antibodies were formulated in 10 mM sodium acetate, 9% sucrose, pH 5.2.

Novel Fc-region loop insertion variants ("loop insertions") with enhanced FcRn binding were engineered with the aid of yeast display technology and incorporated into the IgG2 Fc heavy chain domain 3 regions of mAb2 and mAb3. A double-stranded DNA cassette, C-L5, encoding a combinatorial library of GGC-XXXXXX-CGG was constructed by a standard cloning method, where X was any naturally occurring amino acid (except for cysteine) encoded by the 19 trimer phosphoramidites codon mix (Glen Research, Sterling, VA). The C-L5 cassette was inserted by homologous recombination between N384 and G385 in human IgG1 Fc in a yeast display vector resulting in the L5 Fc library. Diversity was ~$5x10^8$ variants. *S. cerevisiae* yeast cells (~$1.5x10^9$) were incubated with recombinant human FcRn (Amgen, Inc.) and screened by two rounds using magnetic activated cell-sorting (MACS MicroBeads®, Miltenyi Biotec, San Diego, CA) and one round of flow activated cell-sorting (FACS, BD Biosciences, San Jose, CA) at pH 5.5. The screening process produced a population of cells expressing Fc-region that bound FcRn with higher affinity than wild-type Fc at pH 5.5.

A subset of the FACS-sorted yeast was plated, selected, grown, and further analyzed for FcRn binding by FACS. Individual cells showing high affinity to human FcRn at pH 5.5 and low affinity at pH 7.4 were selected. Several peptide variants were identified from the cell screen, and two with high pH 5.5 affinity, designated "8" (-PVLLFN-) and "119" (-AFEFIY-), were shuttled into mammalian expression vectors encoding human IgG2 for incorporation into anti-PCSK9 mAbs. Binding to recombinant cynomolgus monkey FcRn (Amgen, Inc.) was similar to human FcRn for 8 and 119 peptide-containing mAbs (data not shown).

mAb:FcRn Binding Affinity Determination by SPR. Binding of native and Fc-modified mAbs to cynomolgus monkey FcRn was investigated by SPR using a Biacore™ T200

instrument (GE Healthcare Bio-Sciences). Cynomolgus monkey FcRn (10 nM) was pre-mixed with mAb (0.1–2000 nM) in sample buffer containing 10 mM sodium acetate, 150 mM sodium chloride, 0.005% polysorbate 20, and 0.1 mg/ml bovine serum albumin (BSA) at a pH of 5.5. Samples were incubated at room-temperature for 1 h prior to injection over a human Fc surface at a flow rate of 10 μL/min. The Fc surface was generated by immobilizing recombinant human Fc (Amgen, Inc.) on a CM5 chip using amine coupling (~4000 RU). Analyses were run with the Fc surface in the second flow cell, while the first flow cell served as blank control. Sample buffer lacking BSA was used as running buffer. Raw data were collected using BIAevaluation v2.0 software (GE Healthcare Bio-Sciences), and analysis was performed using GraphPad Prism v6 (GraphPad Software, Inc., La Jolla, CA). Uninhibited cynomolgus monkey FcRn binding to human Fc (100% signal) was determined in the absence of mAbs in solution. Decreasing FcRn binding response observed as a consequence of increasing mAb concentrations indicated that FcRn bound to the mAbs in solution, effectively blocking FcRn from binding to immobilized Fc. Plots of the FcRn binding signal versus antibody concentration were analyzed by nonlinear regression (assuming one-site competition) for each mAb to generate EC_{50} values. These values were used as a relative means of comparing Fc-modified and native mAb affinity for cynomolgus monkey FcRn.

Rodent In Vivo Pharmacokinetic and Pharmacodynamic Studies. Male C57Bl/6 mice (*Mus musculus*), 20 weeks of age, were cared for in accordance with the *Guide for the Care and Use of Laboratory Animals* (National Research Council, 2011). Animals were group-housed at an AAALAC-accredited facility in ventilated micro-isolator housing on corn cob bedding. All research protocols were approved by the Institutional Animal Care and Use Committee.

Animals had *ad libitum* access to pelleted feed (Teklad diet #2920, Harlan, Indianapolis, IN) and reverse osmosis-purified water via automatic watering system. Animals were maintained

on a 12 h light/12 h dark photoperiod, and were free of ectoparasites, endoparasites, and known enteric and respiratory pathogens.

A knockout (KO) mouse model was used to investigate the extent to which endogenous PCSK9 played a role in the disposition of mAb1, as measured by relative changes in systemic PK in PCSK9 KO mice compared to C57Bl/6 wild-type (WT) mice. Male KO mice were obtained from Ozgene Pty Ltd (Bentley, Australia), and male WT mice were obtained from Jackson Laboratories (West Sacramento, CA). Serum levels of PCSK9 were determined using an anti-PCSK9 ELISA (R&D Systems, Minneapolis, MN). IgG2 Control or mAb1 was administered to WT and KO animals (n=15/group) via bolus tail vein injection at a dose of 3 mg/kg. Whole blood was collected via tail nick in subsets of animals (n=5) from each group at various time points post-injection (Protocol 1: 15 min and 3, 14, 24, and 42 days; Protocol 2: 4 h and 7, 17, 28, and 49 days; Protocol 3: 24 h and 10, 21, 35, and 56 days), thus each animal was subjected to a maximum of 5 blood collections over a 56 day period (n=5/time point). Blood samples were processed to serum for antibody concentration determination and PK analyses.

The impact of PCSK9 on antibody disposition in vivo was further explored by administering mAb1 to normal mice as a bivalent complex with human PCSK9. The mAb1:PCSK9 complex (1:2 stoichiometry) was generated in vitro using recombinant proteins and isolated prior to in vivo dosing, as described above. Either mAb1:PCSK9 complex or mAb1 alone, as a control, was administered intravenously to male C57Bl/6 mice via bolus tail vein injection at molar equivalent doses of mAb1 (20 or 10 mg/kg, respectively). Blood samples (n=5/time point) were collected at 1, 6, 10, 24, 48, and 96 h and 7, 10, 14, and 21 days, with processing to serum for mAb1 concentration determination and PK analyses. Relative changes in systemic mAb1 PK when dosed as a complex or alone served as an indicator of the influence of exogenous human PCSK9 on antibody disposition.

Non-Human Primate In Vivo Pharmacokinetic and Pharmacodynamic Studies. Male cynomolgus monkeys (*Macaca fascicularis*), weighing 2–5 kg, were cared for in accordance with the *Guide for the Care and Use of Laboratory Animals* (National Research Council, 2011). Animals were housed individually at an indoor, AAALAC-accredited facility. All research protocols were approved by the Institutional Animal Care and Use Committee.

Animals were fed PMI Certified Primate Diet #5048 (Richmond, IN) daily in amounts appropriate for the age and size of the animals, and had *ad libitum* access to water processed through a reverse osmosis filter and delivered via automatic watering system. Animals were maintained on a 12 h light/12 h dark photoperiod in rooms at 64 to 84°F (30 to 70% humidity) and had access to enrichment opportunities. All animals were negative for simian retrovirus.

Non-human primates were utilized as an in vivo model to investigate anti-PCSK9 antibody pharmacokinetics and LDL-C pharmacodynamics. Data presented herein were generated in three separate single-dose studies. In Study 1, mAb1, mAb2, mAb3, mAb4, and IgG2 Control antibodies were administered subcutaneously at a 0.5 mg/kg dose to naïve male monkeys (n=5/group). Subjects were randomized and placed into treatment groups based on body weight and serum LDL-C level measured eight days prior to dosing. Following a pre-dose blood collection, antibodies were dosed and additional blood samples collected at 24, 48, 72, 96, 144, 216, 288, 360, 432, 504, 576, 648, 720, 792, 864, 936, 1008, 1080, 1152, and 1224 h. Blood was processed to serum and stored at -80°C pending shipment to Amgen for PK and PD analyses. The in-life portion of the study was conducted at Valley Biosystems (West Sacramento, CA). In Study 2, mAb1, mAb1_YTE, mAb1_LS, mAb2, mAb2_YTE, and mAb2_LS were administered intravenously at a dose of 1 (mAb2 and variants) or 3 mg/kg (mAb1 and variants) via slow bolus injection to naïve male monkeys (n=4/group). Subjects were randomized and placed into treatment groups based on serum LDL-C level measured nine days prior to dosing. Following a pre-dose blood collection, antibodies were administered and blood

samples collected 0.25, 1, 4, 8, 12, 24, 72, 168, 240, 336, 408, 504, 576, 672, 744, 840, 1008, 1176, and 1344 h for PK. Sampling was the same for PD with the exception of pre-dose, 0.25, 4, and 12 h time points, which were omitted. Blood was processed to serum and stored at -80°C pending antibody concentration determination and PK analysis at Amgen. The in-life phase of the study and LDL-C analysis were performed by Charles River Laboratories (Reno, NV). In Study 3, mAb2, mAb2_8, mAb2_119, mAb3, mAb3_8, and mAb3_119 were administered intravenously at a dose of 1 mg/kg via slow bolus injection to naïve male monkeys (n=4/group). Subjects were randomized and placed into treatment groups based on serum LDL-C level measured seven days prior to dosing. After a pre-dose collection, antibodies were administered and blood samples were collected at 0.25, 1, 4, 8, 12, 24, 72, 168, 240, 336, 408, 504, 576, 672, 744, 840, 1008, 1176, 1344, 1512, and 1680 h for PK. Sampling was the same for PD with the exception of 8 and 12 h time points, which were omitted. Blood was processed to serum and stored at -80°C pending antibody concentration determination and PK analysis at Amgen. The in-life phase of the study and LDL-C determinations were conducted at Charles River Laboratories.

Antibody Pharmacokinetics. Serum concentrations of antibodies dosed to mice and non-human primates were determined by immunoassay using either a plate-based sandwich ELISA method or a microfluidic assay with fluorescent detection on a Gyrolab™ xP workstation (Gyros AB, Uppsala, Sweden). A polyclonal goat anti-human IgG and horseradish peroxidase labeled goat anti-human IgG (Jackson ImmunoResearch Laboratories, Inc., West Grove, PA) were used for analysis of mouse study samples. Cynomolgus monkey study samples were analyzed using a mouse anti-human Fc mAb and a horseradish peroxidase or Alexa647 labeled anti-human Fc mAb (Amgen, Inc.). Analyte concentrations were determined in Watson LIMS™, v7.4 (Thermo Fisher Scientific, Waltham, MA), from data regression of optical density measurements derived from HRP-mediated colorimetric reactions or fluorescence values derived from Alexa647

JPET Fast Forward. Published on February 4, 2015 as DOI: 10.1124/jpet.114.221242
This article has not been copyedited and formatted. The final version may differ from this version.

fluorescence emissions converted to concentration values. Quantitation was based on a 4-parameter logistic ($1/Y^2$) regression of separately prepared standard curves. The lower limit of quantification (LLOQ) for the assays ranged from 34.4 to 48.8 ng/mL. Graphical presentation of mean concentration-time data (±SD) were prepared using SigmaPlot, v12.5 (Systat Software, Inc., San Jose, CA). Individual serum concentrations reported as below the LLOQ were set to zero for the purpose of calculating a mean value. Mean values were calculated if ≥50% of the observations were greater than the LLOQ.

Pharmacokinetic analysis of mouse concentration data obtained from PCSK9 KO and WT mice was performed using Phoenix™ WinNonlin®, v6.0.3.395 (Pharsight, Cary, NC). AUC_{last} (area under the serum concentration-time curve from time zero to the time of last quantifiable concentration), AUC_{inf} (AUC from zero to infinite time), CL (systemic clearance), V_{ss} (volume of distribution at steady-state), and $t_{1/2,z}$ (apparent terminal half-life associated with λ_z) were determined by non-compartmental analysis (NCA). Areas were estimated by linear trapezoidal linear/log interpolation, and $t_{1/2,z}$ was calculated from 504 h (21 d) to either 1008 h (42 d; mAb1 in WT mice) or 1344 h (56 d). Due to the composite study design with intermittent sampling of each animal, pharmacokinetics were calculated based on mean concentrations (n=5) for each time point. Parameters are reported to three significant figures, except for $t_{1/2,z}$ which was reported to two significant figures.

Pharmacokinetic analyses of monkey concentration data obtained from Studies 1-3 were performed in Watson LIMS™ v7.4. In cases where doses were administered intravenously (Studies 2 and 3), the same pharmacokinetic parameters were determined as described previously for mouse. For subcutaneous administration (Study 1), CL/F (apparent clearance) and C_{max} (maximum observed antibody concentration) were calculated. Areas were estimated by the linear log-linear trapezoidal method, and $t_{1/2,z}$ was estimated during the log-linear terminal phase of the concentration-time profiles. All parameters were determined by NCA for individual

JPET Fast Forward. Published on February 4, 2015 as DOI: 10.1124/jpet.114.221242
This article has not been copyedited and formatted. The final version may differ from this version.

animals, and mean values (±SD) were reported for each dose group (two significant figures for $t_{1/2,z}$ and three significant figures for all other parameters). Within each study, one way ANOVA was performed using SigmaPlot to determine if clearance and half-life differed by treatment (pH-sensitive PCSK9 binding or enhanced FcRn binding). When significance was established (alpha=0.05), a pairwise multiple comparison was performed using the Holm-Sidak method.

Given the pharmacology of PCSK9 and its role in trafficking LDLR to the lysosome (Lagace et al., 2006), it was initially hypothesized that anti-PCSK9 antibodies would be subjected to TMD and exhibit dose-dependent changes in CL. The impact of PCSK9 target on mAb PK was subsequently confirmed in mice (described herein) and in cynomolgus monkeys (data not shown). Similar findings were recently described (Chaparro-Riggers et al., 2012). As the aims of the present investigation were specifically to explore relative differences in AUC exposure, CL, and apparent half-life between antibodies of varying target and FcRn affinity, an NCA approach was used to characterize antibody pharmacokinetics for comparison at identical doses. Differences in these parameters between antibodies were taken as evidence of influence of the target or FcRn on antibody disposition. AUC_{last} and AUC_{inf} were reported as a means to judge the extent to which exposure (and therefore CL) was effectively captured using the NCA approach.

PCSK9 and LDL-C Pharmacodynamics. Serum levels of total PCSK9 at selected time points were measured using a Quantikine human PCKS9 immunoassay kit (R&D Systems). The assay had good accuracy and precision, and was qualified with an LLOQ of 1 ng/mL. Serum LDL-C was measured colorimetrically using either a Cobas Integra® 400 (Roche Diagnostics Corporation, Indianapolis, IN) or Olympus AU640e® (Olympus Corporation, Center Valley, PA) clinical chemistry analyzer. Graphical presentation of mean PCSK9 and LDL-C data (±SEM) were prepared using SigmaPlot. Determination of the maximal LDL-C lowering (E_{max}) for individual subjects was made by calculating the difference between the lowest observed

LDL-C level achieved post-treatment and the corresponding LDL-C baseline, established by taking the mean of the day -8 or -9 and time 0 pre-dose values (Studies 1 and 3). LDL-C baseline for Study 2 was taken to be the day -7 value, since the time 0 pre-dose samples were not analyzed for PD. Overall pharmacological effect for individual subjects was assessed by calculating the LDL-C effect curve area (ECA). Baseline values as described above for individual subjects in each study were multiplied by the study sampling duration to define the baseline area ($A_{baseline}$). Area under the LDL-C effect profiles (A_{NCA}) was then estimated by NCA in Phoenix™ WinNonlin® using the trapezoidal method with linear interpolation. The difference between $A_{baseline}$ and A_{NCA} was the LDL-C ECA ($A_{baseline}$-A_{NCA}=ECA). Individual values of E_{max} and ECA in each dose group were used to calculate mean values (±SEM).

Statistical analyses were performed on the LDL-C pharmacodynamic data to evaluate if pH-sensitive PCSK9 binding or enhanced FcRn binding resulted in: 1) increased E_{max} or ECA; or 2) difference in LDL-C lowering time course. SAS® for Windows Vista (Release 9.2, SAS Institute, Cary, NC) was used for the analyses, with inferential statistical tests conducted at the 5% level. The statistical methods were consistent across the three cynomolgus monkey studies and are described below.

An analysis of variance model was used to evaluate the effect of treatments (pH-sensitive PCSK9 binding or enhanced FcRn binding) on E_{max} and ECA. Data were log-transformed prior to the statistical analysis. A one-way homoscedastic ANOVA model (allowing for a common variance for all groups) and a one-way heteroscedastic ANOVA model (allowing for a different variance in each group) were compared, and the one with the lower AIC value was chosen for analysis. The Kenward and Roger's method for calculation of degrees of freedom was used for inferential test statistics.

A repeated measure analysis of covariance (baseline as covariate) model was first used to evaluate the effect of treatments (pH-sensitive PCSK9 binding or enhanced FcRn binding) on

the time course of LDL-C reduction. LDL-C was log-transformed prior to the statistical analysis. Variance and covariance structure of the repeated measures was selected on the basis of lowest Akaike Information Criterion (AIC) among commonly used covariance structures, including compound-symmetry (CS), heterogeneous compound symmetry (CSH), first-order autoregressive (AR(1)), and heterogeneous first-order autoregressive (ARH(1)). The Kenward and Roger's method for calculation of degrees of freedom was used for the inferential test statistics. The effect of treatment group, effect of time, and the interaction between treatment group and time were estimated by the model. Comparisons among treatment groups at each post-dose time point, and comparisons between the post-dose and pre-dose time points, were performed only when the interaction between treatment group and time was statistically significant, implying treatment-dependent time courses. The multiple comparisons among treatment groups were not adjusted. The multiple comparisons between post-dose and pre-dose time points were adjusted by multiplying the p-value by the square-root of the number of post-dose time points.

JPET Fast Forward. Published on February 4, 2015 as DOI: 10.1124/jpet.114.221242
This article has not been copyedited and formatted. The final version may differ from this version.

Results.

Pharmacokinetics of mAb1 in PCSK9 WT and KO Mice. PK studies were performed in PCSK9 WT and KO mice with mAb1 (K_D=0.160 nM for mouse PCSK9) to evaluate the impact of target antigen on the systemic exposure of a high-affinity mAb (Chan et al., 2009). The serum concentration of endogenous PCSK9 in C57Bl/6 WT mice was 70.9±41.1 ng/mL (mean±SD; n=10), or ~1 nM, as measured by ELISA. No PCSK9 protein was detectable in PCSK9 KO mice (n=5), confirming that the model was a valid tool for assessing mAb1 PK in the absence of PCSK9. Similar to results reported previously for antibody J10 (Chaparro-Riggers et al., 2012), the mAb1concentration-time profile in WT mice differed greatly from that observed in PCSK9 KO mice (Figure 1A). Systemic CL of mAb1 was ~4-times higher and terminal half-life was ~4-times shorter in the presence of PCSK9 than in its absence (Table 1). AUC, CL, and half-life of mAb1 in KO mice were all similar to IgG2 Control values in both WT and KO mice, emphasizing that inherent instability or other pharmacologic liability were not likely responsible for the unique mAb1 PK behavior in the WT strain.

Additionally, administration of mAb1 to WT mice in the form of an immune complex with exogenous (human) PCSK9 allowed for exploration of the effect of antigen on mAb1 PK at higher mAb doses (equivalent to 10 mg/kg), where impact of TMD is otherwise expected to be minimal. The PK profile of mAb1 administered as complex varied significantly from that of mAb1 alone at an equivalent antibody dose (Figure 1B). Systemic CL of mAb1 dosed as a complex was higher than mAb1 dosed alone by a factor of ~11 (Table 1). Immunoassay detection of mAb1 dosed as mAb1:PCSK9 complex relied on reagents specific for human Fc, therefore the resulting mAb1 PK profile could potentially reflect multiple mAb1 species, PCSK9-bound or unbound. Overall, results from both mouse studies provided clear evidence of a role for PCSK9 in the disposition of neutralizing mAbs.

JPET Fast Forward. Published on February 4, 2015 as DOI: 10.1124/jpet.114.221242
This article has not been copyedited and formatted. The final version may differ from this version.

Determination of Antibody Fab:PCSK9 Binding Kinetics and Affinities by SPR. Kinetic data resulting from SPR analyses of mAb1–4 Fab binding to cynomolgus monkey PCSK9 at pH 7.4 and 5.5 (Supplemental Figure 1) demonstrated varying degrees of pH-sensitivity across the panel of Fabs (Table 2). Data indicated that mAb1 Fab bound PCSK9 with high affinity under both pH conditions (K_D=0.00596 and 0.0102 nM at pH 7.4 and 5.5, respectively). This similarity in K_D values suggested that antigen binding was not affected by pH, as association rate constants were identical at both pHs and dissociation rate constants differed by a factor of <2. mAb2 Fab bound PCSK9 with lower affinity (K_D=4.55 nM at pH 7.4) compared to mAb1 Fab as a result of reduced k_a (~10-times lower) and increased k_d (~80-times higher). In contrast to mAb1 Fab, mAb2 Fab exhibited pH-dependent PCSK9 binding. At pH 5.5, a modest reduction in k_a (<3-times) was observed compared to pH 7.4, while k_d increased by a factor of 60 from 11.2×10^{-4} to 670×10^{-4} s^{-1}, resulting in a K_D of 676 nM. The mAb2 Fab pH 5.5 k_d corresponds to a complex dissociation half-life of 10 s, which was substantially different from the mAb1 Fab complex dissociation half-life of 28000 s. Binding kinetics of mAb4 Fab were generally comparable to mAb2 Fab; PCSK9 binding was pH-dependent, and the k_d at pH 5.5 translated to a similar complex dissociation half-life (13 s). Subtle differentiation between mAb4 and mAb2 Fab was observed with regard to affinity, where mAb4 Fab bound PCSK9 with higher affinity at pH 7.4 and 5.5 (K_D=0.979 and 292 nM, respectively). mAb3 Fab exhibited higher affinity than mAb4 Fab at pH 7.4 and 5.5 (K_D=0.166 and 54.2 nM, respectively), but lower affinity compared to mAb1 Fab. Based upon $k_{d,5.5}/k_{d,7.4}$ and $K_{D,5.5}/K_{D,7.4}$ ratios calculated for each Fab, mAb3 had the highest degree of pH-dependent binding, followed by mAb4, mAb2, and mAb1 Fab. However, the pH 5.5 mAb3 Fab k_d value of 88.7×10^{-4} s^{-1} translated to a complex dissociation half-life of 78 s, which was longer than mAb2 and mAb4 Fab. Overall, the diverse range of PCSK9 binding characteristics represented by the panel of antibodies warranted investigation in vivo to assess relative impact on pharmacokinetic attributes and LDL-C outcomes.

JPET Fast Forward. Published on February 4, 2015 as DOI: 10.1124/jpet.114.221242
This article has not been copyedited and formatted. The final version may differ from this version.

Pharmacokinetics of pH-Sensitive Antibodies and LDL-C Pharmacodynamics in Monkeys. The effects of pH-sensitive PCSK9 binding on PK and PD responses, measured by changes in total PCSK9 and reduction in LDL-C relative to baseline levels, were evaluated in cynomolgus monkeys. Mean concentration-time profiles (±SD) for mAb1, mAb2, mAb3, mAb4, and IgG2 Control are shown in Figure 2A, mean concentration-time profiles for total PCSK9 (±SEM) are displayed in Figure 2B, and mean LDL-C pharmacodynamic profiles (±SEM) are presented in Figure 2C. Mean pharmacokinetic and pharmacodynamic data, as described in the Methods, are summarized in Table 3. Summaries of the p-values resulting from pairwise comparison of CL/F and $t_{1/2,z}$ and the adjusted p-values for LDL-C difference from baseline are presented in the Supplemental Data section (Supplemental Tables 1 and 2, respectively). Statistical analyses indicated that LCL-C profiles differed across treatments.

PK properties of the IgG2 Control were consistent with expectation for a human antibody dosed to monkeys, based on observed CL/F (0.128 mL/h/kg) and $t_{1/2,z}$ (460 h). Notably, mAb1 CL/F (1.37 mL/h/kg) was 11-times higher than IgG2 Control, and half-life (49 h) was 9-times shorter. The LDL-C effect curve area (ECA) was 422 mg·d/dL, which differed significantly from mAb2, mAb3, and mAb4 ECA estimates (pairwise comparison p-values ranged from 0.002-0.015). The duration of LDL-C reduction (defined as the last time point at which LDL-C differed from pre-dose baseline) for mAb1 was 6 d, shorter than all other antibodies dosed in the study. mAb2 AUC exposure (4180 µg·h/mL), CL/F (0.123 mL/h/kg), and $t_{1/2,z}$ (340 h) were profoundly different from mAb1, exhibiting unexpected similarity to values attributed to pharmacologically inactive IgG2 Control (Supplemental Table 1). Despite PK behavior seemingly unaffected by target-binding, mAb2 duration of LDL-C lowering was 51 d (9-times longer than mAb1) with an ECA of 1230 mg·d/dL (3-times higher than mAb1). mAb4 CL/F was modestly higher (0.249 mL/h/kg) and half-life was somewhat shorter (250 h) compared to mAb2, but these differences were not statistically significant. The duration of action for mAb4 (39 d) was shorter than mAb2,

but its ECA (1320 mg·d/dL) was similar. Lastly, mAb3 CL/F (0.432 mL/h/kg) and half-life (150 h) fell in a range between those of mAb4 and mAb1. Not unexpectedly, the observed duration of LDL-C lowering (18 d) and ECA (925 mg·d/dL) for mAb3 also fell in a range between mAb4 and mAb1. Overall, these results established a correlation between antibody exposure (AUC) and degree of pharmacological effect (ECA). In addition, longer apparent terminal half-life was consistently associated with longer duration of LDL-C lowering. Though mAb1 ECA differed significantly from the other anti-PCSK9 antibodies, mAb2, mAb3, and mAb4 ECAs were not statistically distinguishable from one another. Statistical analysis of LDL-C data at each time point revealed differentiation between mAb2 and mAb3 at just more than half the time points (13); comparison of mAb2 with mAb4 and mAb3 with mAb4 showed differentiation at less than half the time points (3 and 8, respectively). E_{max} values ranged from 37-47 mg/dL across the four dose groups, and no statistical differences between groups were observed. Where duration of action differed widely across the antibodies tested, differences in maximum degree of LDL-C reduction at the nadir were not detected.

Total serum PCSK9 concentrations were elevated and returned to near pre-dose levels in a time course similar to LDL-C for mAbs1–4 (Figure 2B). The increase in antigen levels was generally consistent with effects observed for other mAbs neutralizing soluble targets (Davda and Hansen, 2010). This indicated that target engagement by the antibodies was associated with the pharmacological response. The degree of PCSK9 increase was variable across the antibodies, suggesting the magnitude of increase may be a function of differential antigen affinity.

Relative Anti-PCSK9 Antibody Fc Binding Affinities for Cynomolgus Monkey FcRn. Native mAbs and Fc-variants containing modifications to enhance FcRn binding affinity were subjected to competitive binding analysis prior to dosing in monkeys. EC_{50} values used to

compare relative mAb Fc affinities for cynomolgus monkey FcRn at endosomal pH (5.5) are presented in Table 4. Native mAb1, mAb2, mAb3, and mAb4 EC_{50}s were reasonably comparable, ranging from 83.7–210 nM. This result was not unexpected, since the antibody IgG2-derived Fc sequences were the same. Therefore, variability in the CDRs responsible for evoking different PCSK9 binding properties appeared to have limited impact on FcRn binding, though interesting examples where Fab variation did affect FcRn binding have been described (Wang et al., 2011). Similarly, mAb binding to PCSK9 did not seem to affect mAb interaction with FcRn, as experiments conducted with mAb1:PCSK9 complex indicated that human FcRn affinity was comparable to mAb1 alone (data not shown).

Fc-variants of mAb1 that incorporated the previously described YTE and LS amino acid substitutions (see Materials and Methods) exhibited EC_{50}s of 6.48 and 16.1 nM, respectively, which corresponded to increases in FcRn affinity by a factor of 7–16 compared to native mAb1. Likewise, FcRn affinities of mAb2_YTE and mAb2_LS improved by a factor of 7–11 relative to native mA2. In both examples, YTE mutations resulted in modestly larger affinity improvements relative to the LS mutations, and this improvement was not influenced meaningfully by CDR sequence. The novel Fc loop-insertion variants, 8 and 119, afforded a greater shift in FcRn binding affinity in mAb2 than the YTE and LS point mutations. mAb2_8 and mAb2_119 EC_{50}s (3.09 and 4.44 nM, respectively) were 68- and 48-times lower than the native mAb2 EC_{50} (209 nM) measured in the same experiment. The 8 and 119 loop-insertion variants of mAb3 exhibited 3.59 and 3.62 nM EC_{50} values, respectively, which corresponded to an affinity improvement on the order of 35-times compared to native mAb3. An in vitro assessment of FcRn affinities at pH 7.4 confirmed no FcRn binding or significantly reduced binding, as EC_{50}s either could not be determined under the conditions of the assay or were ~100–1000-times higher (right-shifted) than at pH 5.5 (data not shown). In vitro pH 5.5 FcRn binding

JPET Fast Forward. Published on February 4, 2015 as DOI: 10.1124/jpet.114.221242
This article has not been copyedited and formatted. The final version may differ from this version.

improvements offered by the panel of Fc variants were sufficient to warrant further investigation in vivo to assess impact on antibody PK and PD responses.

Pharmacokinetics of Fc-Variant Antibodies and LDL-C Pharmacodynamics in Monkeys. The effects of enhanced FcRn binding on PK and PD responses, measured by reduction in LDL-C relative to baseline levels, were evaluated in cynomolgus monkeys for mAbs of varying PCSK9 affinity. Mean concentration-time profiles (±SD) for mAb1, mAb1_YTE, mAb1_LS, mAb2, mAb2_YTE, and mAb2_LS are shown in Figure 3A, and mean LDL-C pharmacodynamic profiles (±SEM) are presented in Figure 3B. Mean pharmacokinetic and pharmacodynamic data, as described in Materials and Methods, are summarized in Table 3. Summaries of the p-values resulting from pairwise comparison of CL/F and $t_{1/2,z}$ and the adjusted p-values for LDL-C difference from baseline are presented in the Supplemental Data section (Supplemental Tables 3 and 4, respectively). Statistical analyses indicated that LCL-C profiles differed across treatments.

For native mAb1, systemic CL (0.683 mL/h/kg) was similar to the CL observed for YTE and LS variants (0.650 and 0.684 mL/h/kg, respectively). Likewise, half-life estimates were similar across the three antibodies, ranging from 42-52 h. No statistical difference was detected in CL or half-life when comparing mAb1 with either variant. LDL-C pharmacodynamic profiles for mAb1 and its YTE and LS Fc variants were overlaid, with similar ECA values observed and identical durations of LDL-C lowering (10 d) for each. The mAbs exhibited no statistical difference in LDL-C lowering throughout the time course. These results demonstrated that improved FcRn binding had no meaningful impact on PK or PD for a high affinity, pH-insensitive PCSK9-binder. For mAb2, with lower, pH-sensitive affinity, some degree of differentiation was observed between native antibody and the YTE and LS Fc point mutants with regard to CL and half-life. mAb2_YTE and mAb2_LS exhibited CL of 0.0931 and 0.118 mL/h/kg, respectively, compared to 0.168 mL/h/kg for native mAb2; however, this reduction in CL was not great

enough to achieve statistical significance (Table S3). Estimates of half-life for mAb2_YTE and mAb2_LS (470 and 420 h, respectively) were <2-times longer than mAb2 (270 h). With regard to pharmacodynamic endpoints, the YTE and LS Fc point mutants exhibited similar E_{max} values compared to native mAb, with ECAs trending higher for YTE and LS than for native mAb2. Though E_{max} and ECA differences were not significant, statistical analysis of the duration of LDL-C lowering showed a modest prolongation of PD effect for both mAb2_YTE and mAb2_LS (42 and 56 d, respectively) compared to mAb2 (35 d). Statistical differentiation between the LDL-C time courses of mAb2 and both the YTE and LS Fc-variants occurred at only 2–3 time points.

Mean concentration-time profiles (±SD) for mAb2, mAb2_8, mAb2_119, mAb3, mAb3_8, and mAb3_119 are shown in Figure 4A, and mean LDL-C pharmacodynamic profiles (±SEM) are presented in Figure 4B. Mean pharmacokinetic and pharmacodynamic data, as described in the Methods, are summarized in Table 3. Summaries of the p-values resulting from pairwise comparison of CL/F and $t_{1/2,z}$ and the adjusted p-values for LDL-C difference from baseline are presented in the Supplemental Data section (Supplemental Tables 5 and 6, respectively). Statistical analyses indicated that LDL-C profiles differed across treatments.

For native mAb3, systemic CL (0.634 mL/h/kg) was significantly higher compared to CL observed for 8 and 119 Fc loop-insertion mutants (0.422 and 0.381 mL/h/kg, respectively; p-values <0.001). Estimates of $t_{1/2,z}$, however, were similar across the three antibodies, ranging from 120-150 h. LDL-C pharmacodynamic profiles for mAb3_8 and mAb3_119 showed some degree of differentiation from native mAb3, though fewer than 5 LDL-C observations between the native mAb and either loop variant were statistically different. ECAs for the loop variants were not statistically distinguishable from mAb3, and no change in E_{max} was observed. When duration of LDL-C was assessed for each mAb3 antibody, pharmacological effect was extended for both Fc loop-insertion variants (18 d) compared to the native form (11 d). These results

demonstrated that improved FcRn binding for mAb3 (an antibody with moderate pH-sensitive PCSK9 affinity) resulted in a meaningful reduction in CL with extension of pharmacological effect, though differences in antibody half-lives and ECAs were not significant. mAb2_8 and mAb2_119 exhibited CL of 0.147 and 0.217 mL/h/kg, respectively, compared to 0.222 mL/h/kg for native mAb2. Unlike the 8 and 119 variants of mAb3, however, this reduction in CL was not great enough to achieve statistical significance (Supplemental Table 5). Estimates of half-life for mAb2_8 and mAb2_119 (430 and 200 h, respectively) were both within a factor of 2 of the native form (250 h). In terms of pharmacodynamic endpoints, the 8 and 119 Fc loop-insertion variants showed no change in E_{max} compared to native mAb2, with ECAs trending higher for 8 and 119. Though E_{max} and ECA differences were not significant, statistical analysis of the duration of LDL-C lowering suggested a modest prolongation of PD effect for both mAb2_8 and mAb2_119 (43 d) compared to mAb2 (36 d). Generally, incorporation of the Fc point mutants (YTE and LS) and the Fc loop-insertion variants (8 and 119) into mAb2 revealed similar PK and PD attributes that delivered modest improvements compared to native mAb2. Differences were difficult to definitively establish given the statistical power of these in vivo studies.

JPET Fast Forward. Published on February 4, 2015 as DOI: 10.1124/jpet.114.221242
This article has not been copyedited and formatted. The final version may differ from this version.

Discussion.

Therapeutic antibodies that bind cell-surface antigens subject to internalization are known to exhibit non-linear pharmacokinetics that can be attributed to disposition mediated by target antigen (Levy, 1994). While TMD is generally anticipated for drug targets expressed at the cell surface, a potential role for soluble targets to contribute to antibody clearance is less well-established (Body et al., 2006; Deng et al., 2012; Tabrizi et al., 2010). PCSK9, a secreted soluble protein, down-regulates LDLR by directing it to the lysosome for degradation following cellular uptake, thereby reducing endosomal recycling of LDLR. This pathway likely involves APLP2, which recently has been identified as a PCSK9 binding partner responsible for enhanced lysosomal distribution of PCSK9:LDLR complex (DeVay et al., 2013). Given the function of PCSK9 with regard to LDLR down-regulation, it follows that PCSK9:mAb complex formation would serve as a clearance pathway for a therapeutic mAb with high PCSK9 affinity, as recently confirmed (Chaparro-Riggers et al., 2012).

Results from the mAb1 mouse PK studies (Figure 1) clearly demonstrate that antibody association with PCSK9 leads to increased clearance and reduced systemic exposure. While IgG2 Control pharmacokinetics are similar in WT and PCSK9 KO mice, mAb1 AUC in WT mice is only 27% of the AUC observed in KO mice, where PCSK9 is absent (Table 1). These results are consistent with those reported recently for a different anti-PCSK9 mAb (Chaparro-Riggers et al., 2012). Furthermore, mAb1 mouse exposure observed upon administration of bivalent mAb1:PCSK9 complex is only 9% of the exposure achieved by administration of mAb1 alone at an equivalent dose. While the mouse model allows for a general characterization of PCSK9-mediated TMD in vivo, it offers limited utility for detailed investigation of how mAbs engineered to have reduced TMD will perform with respect to extent and duration of LDL-C reduction and translation thereof to human. This is largely due to the fact that the lipoprotein profile in mice consists primarily of HDL-C, whereas LDL-C is a more significant component in human and

non-human primates (Getz and Reardon, 2012). Mouse serum PCSK9 levels, 50–150 ng/mL, are also lower than human and non-human primate levels of 250–500 ng/mL (Chan et al., 2009; Lagace et al., 2006; Tavori et al., 2013). Collectively, these factors afford a rationale for utilizing non-human primates to investigate mAb:PCSK9 binding attributes that deliver optimal mAb exposure profiles and pharmacological responses.

A panel of four anti-PCSK9 mAbs has been evaluated for PK properties and LDL-C lowering in monkeys. Due to sequence variation within the CDRs, antigen affinities differ greatly at pH 7.4 across the panel, with K_D values in the range of 0.00596–4.55 nM (Table 2). This variation in PCSK9 affinity gives rise to notable relative differences between antibodies with respect to both PK and PD profiles (Figure 2). A ranking of mAbs based on increasing exposure and duration of LDL-C reduction (Table 3) produces a rank-order, mAb1<mAb3<mAb4<mAb2, identical to that generated when antibodies were ranked according to increasing K_D. PCSK9 affinity at pH 7.4 is, therefore, inversely correlated with both antibody exposure and duration of LDL-C lowering within the K_D range explored. As expected, the IgG2 Control mAb exhibits no pharmacological effect. Thus, one anticipates a point at which the relationship between lower affinity and increased duration of effect must reverse, as eventually binding will be too weak to effectively neutralize PCSK9. Based on the range of K_D values represented in the mAb panel, this transition likely occurs at some undetermined point beyond the upper K_D bound of ~5 nM.

Since antigen dissociation in the endosomal environment is hypothesized to prolong mAb exposure and maximize the duration of LDL-C reduction, PCSK9 binding affinity at pH 5.5 is also a variable of significant interest. With the exception of mAb1, which has similar affinity at both pH 7.4 and 5.5 (0.00596 and 0.0102 nM, respectively), the panel of antibodies exhibits lower affinity at endosomal pH compared to serum pH ($K_{D,5.5}/K_{D,7.4}$=150–330 for mAbs2–4). In the absence of pH-dependent antigen binding, mAb1 AUC (370 μg·h/mL) and duration of LDL-C

reduction (6 d) are markedly lower than the other mAbs (Table 3). By comparison, mAb2 ($K_{D,5.5}$=676 nM) and mAb4 ($K_{D,5.5}$=292 nM) AUCs are 11- and 6-times higher, and LDL-C reductions are 45 and 33 days longer than mAb1, respectively. Though mAb3 demonstrates the greatest degree of pH-sensitive PCSK9 binding ($K_{D,5.5}/K_{D,7.4}$=330), its PK and PD attributes are less favorable relative to mAb2 and mAb4. Prioritization of mAb candidates should, therefore, be based on a careful assessment of the association and dissociation rate constants that are determinants of K_D, in addition to $K_{D,5.5}/K_{D,7.4}$ ratio. Optimal attributes are likely target-dependent.

An examination of the antigen binding kinetics driving mAb affinity at pH 5.5, particularly the dissociation rate constants (k_d), reveals that mAb:PCSK9 complex dissociation rates relative to endosomal recycling timeframe is a more accurate predictor of activity duration than $K_{D,5.5}/K_{D,7.4}$ ratios. Dissociation half-lives ($t_{1/2,dis}$) of 10 and 13 s at pH 5.5 for mAb2 and mAb4, respectively, are shorter compared to those for mAb3 (78 s) and, particularly, mAb1 (28000 s), as shown in Table 2. Ranking of the four antibodies based on increasing complex dissociation half-life at endosomal pH produces an order, mAb2<mAb4<mAb3<mAb1, that is exactly the reverse rank-order as that generated previously (mAb1<mAb3<mAb4<mAb2) based on increasing exposure and duration of pharmacological effect. The inverse correlation strongly supports the contention that more rapid dissociation of PCSK9:antibody complex leads to a reduction in antibody CL and prolongation of LDL-C lowering.

The process of endosomal recycling has been studied looking at transferrin receptor mediated processing of transferrin, indicating that the intracellular half-life of recycled transferrin is ~7.5 min (Hopkins and Trowbridge, 1983). These results are consistent with the dynamics of FcRn-mediated salvage of IgG evaluated by live cell imaging of FcRn-green fluorescent protein (Ober et al., 2004). Based on these data, a total transit time of ~11 min (intracellular half-life/ln2) for endosomal sorting has recently been proposed (Chen and Balthasar, 2012), which is

JPET Fast Forward. Published on February 4, 2015 as DOI: 10.1124/jpet.114.221242
This article has not been copyedited and formatted. The final version may differ from this version.

expected to apply to neutralizing anti-PCSK9 antibodies that dissociate from the soluble target in the acidified endosome. In the present study, differentiation in PK and PD between mAb4 and mAb3 ($t_{1/2,dis}$=13 and 78 s, respectively) implies that endosomal dissociation half-lives under 20 s may be desirable.

Engineering of anti-PCSK9 mAbs to incorporate Fc-region mutations for enhanced FcRn recycling yields mixed results. mAb1 and mAb2 YTE and LS variants exhibit improved in vitro FcRn binding (7–16-times) relative to their native forms that is comparable to other YTE or LS variant mAbs (Kuo and Aveson, 2011). Despite this improvement, mAb1 variants display little discernable PK benefit and unaltered PD response (Figure 3), suggesting any enhancement in FcRn recycling is masked by TMD. For mAb2, where the role of TMD is minimized due to pH-sensitive PCSK9 binding, PK and PD profiles of YTE and LS Fc-variants reveal only modest improvement: systemic CL, terminal half-life, ECA, and E_{max} are not statistically differentiable from native mAb2 (Table 3). Overall duration of response for the Fc-variants, however, appears to be increased by 7–21 days. This apparent discord may be related to variability in LDL-C concentrations as they return to pre-dose levels in the native mAb2 group, where a “spike” observed on day 49 (Figure 3B) resulted in a more abrupt termination of PD effect for the native mAb than for either Fc-variant (where such an effect was not obvious). The collective data for mAb2 suggest enhanced FcRn binding conferred by YTE and LS Fc mutations do not result in robust enhancement of PD attributes. Interestingly, other examples of YTE and LS incorporation produce greater impact. Bevacizumab and cetuximab variants exhibit statistically differentiable degrees of tumor growth inhibition in mouse xenograft models resulting from antibody exposures that are 5–6-times greater than the native forms (Zalevsky et al., 2010). Since the magnitude of in vivo effect delivered by these Fc-variants appears to be relatively modest in the present study, it raises the question of whether PCSK9 pharmacology renders FcRn binding enhancement approaches less effective.

A new approach to modulate FcRn affinity has been explored through incorporation of novel small peptides into an IgG Fc-region loop that impart enhanced FcRn interactions to the mAb by a means distinct from the Fc point mutations. The extent of in vitro binding improvement for Fc loop-insertion variants 8 and 119 (35–68-times) is higher than for YTE and LS constructs (Table 4). This higher degree of in vitro binding affinity improvement, however, yields similar in vivo results to YTE and LS variants in the context of PCSK9 pharmacology. The 8 and 119 loop variants of mAb3 reveal significant reductions in CL with no effect on half-life (Table 3). An apparent 7-day extension of PD effect is accompanied by no improvement in ECA or E_{max} compared to native mAb3. Incorporation of the same Fc loops into mAb2 results in little discernable PK benefit, though some prolongation of PD effect similar to mAb3 (7 days) is observed. Together, data demonstrate there is no value in Fc engineering efforts to improve FcRn binding for high affinity anti-PCSK9 mAbs, and perhaps only limited value in pursuing this approach for mAbs with pH-sensitive PCSK9 binding.

Overall, data presented here confirm that soluble target pharmacology can be an important determinant of mAb disposition, and emphasize that depending on the nature of the target, mAbs of highest affinity may not exhibit optimal effect in vivo. Observations are consistent with the hypothesis that pH-sensitive target binding enables rapid endosomal dissociation of the mAb:PCSK9 complex, leading to enhancement of LDL-C reduction in cynomolgus monkeys. Further attempts to improve PK and PD by engineering higher FcRn affinity in combination with pH-sensitive PCSK9 binding had little impact compared to modulation of PCSK9 binding alone. Interestingly, however, such an approach showed promise for an anti-IL-6 receptor mAb (Igawa et al., 2010), suggesting success in this approach may be target-dependent. Complete understanding of target biology is critical in designing the optimal therapeutic.

Acknowledgments.

The authors wish to acknowledge Yongmei Di for determination of serum lipids in the non-human primate study analyses conducted at Amgen, and Liming Sui for characterization of total PCSK9 concentrations in serum. Drs. John P. Gibbs and Jasmine P. Davda are acknowledged for their contributions to the manuscript.

JPET Fast Forward. Published on February 4, 2015 as DOI: 10.1124/jpet.114.221242
This article has not been copyedited and formatted. The final version may differ from this version.

Authorship Contributions.

Participated in research design: Henne, Ason, Howard, Wang, Sun, Chan, King, Ketchem, Michaels, Jackson, Retter

Conducted experiments: Henne, Ason, Howard, Wang, Sun, Higbee, Tang, Matsuda, Xu, Chan

Contributed new reagents or analytic tools: Sun, Higbee, Tang, King, Piper, Ketchem

Performed data analysis: Henne, Ason, Howard, Wang, Tang, Xu, Zhou, King, Piper, Ketchem, Michaels, Jackson

Wrote or contributed to the writing of the manuscript: Henne, Jackson, Retter

References.

Abifadel M, Varret M, Rabes JP, Allard D, Ouguerram K, Devillers M, Cruaud C, Benjannet S, Wickham L, Erlich D, Derre A, Villeger L, Farnier M, Beucler I, Bruckert E, Chambaz J, Chanu B, Lecerf JM, Luc G, Moulin P, Weissenbach J, Prat A, Krempf M, Junien C, Seidah NG, and Boileau C (2003) Mutations in PCSK9 cause autosomal dominant hypercholesterolemia. *Nat Genet* **34:** 154-156.

Body JJ, Facon T, Coleman RE, Lipton A, Geurs F, Fan M, Holloway D, Peterson MC, and Bekker PJ (2006) A study of the biological receptor activator of nuclear factor-kappaB ligand inhibitor, denosumab, in patients with multiple myeloma or bone metastases from breast cancer. *Clin Cancer Res* **12:** 1221-1228.

Brown MS, Herz J, and Goldstein JL (1997) LDL-receptor structure. Calcium cages, acid baths and recycling receptors. *Nature* **388:** 629-630.

Careskey HE, Davis RA, Alborn WE, Troutt JS, Cao G, and Konrad RJ (2008) Atorvastatin increases human serum levels of proprotein convertase subtilisin/kexin type 9. *J Lipid Res* **49:** 394-398.

Chan JC, Piper DE, Cao Q, Liu D, King C, Wang W, Tang J, Liu Q, Higbee J, Xia Z, Di Y, Shetterly S, Arimura Z, Salomonis H, Romanow WG, Thibault ST, Zhang R, Cao P, Yang XP, Yu T, Lu M, Retter MW, Kwon G, Henne K, Pan O, Tsai MM, Fuchslocher B, Yang E, Zhou L, Lee KJ, Daris M, Sheng J, Wang Y, Shen WD, Yeh WC, Emery M, Walker NP, Shan B,

Schwarz M, and Jackson SM (2009) A proprotein convertase subtilisin/kexin type 9 neutralizing antibody reduces serum cholesterol in mice and nonhuman primates. *Proceedings of the National Academy of Sciences of the United States of America* **106:** 9820-9825.

Chaparro-Riggers J, Liang H, DeVay RM, Bai L, Sutton JE, Chen W, Geng T, Lindquist K, Casas MG, Boustany LM, Brown CL, Chabot J, Gomes B, Garzone P, Rossi A, Strop P, Shelton D, Pons J, and Rajpal A (2012) Increasing serum half-life and extending cholesterol lowering in vivo by engineering antibody with pH-sensitive binding to PCSK9. *J Biol Chem* **287:** 11090-11097.

Chen Y and Balthasar JP (2012) Evaluation of a catenary PBPK model for predicting the in vivo disposition of mAbs engineered for high-affinity binding to FcRn. *AAPS J* **14:** 850-859.

Cholesterol Treatment Trialists, Baigent C, Blackwell L, Emberson J, Holland LE, Reith C, Bhala N, Peto R, Barnes EH, Keech A, Simes J, and Collins R (2010) Efficacy and safety of more intensive lowering of LDL cholesterol: a meta-analysis of data from 170,000 participants in 26 randomised trials. *Lancet* **376:** 1670-1681.

Cohen JC, Boerwinkle E, Mosley TH, Jr., and Hobbs HH (2006) Sequence variations in PCSK9, low LDL, and protection against coronary heart disease. *N Engl J Med* **354:** 1264-1272.

Dall'Acqua WF, Woods RM, Ward ES, Palaszynski SR, Patel NK, Brewah YA, Wu H, Kiener PA, and Langermann S (2002) Increasing the affinity of a human IgG1 for the neonatal Fc receptor: biological consequences. *J Immunol* **169:** 5171-5180.

Dall'Acqua WF, Kiener PA, and Wu H (2006) Properties of human IgG1s engineered for enhanced binding to the neonatal Fc receptor (FcRn). *J Biol Chem* **281:** 23514-23524.

Davda JP and Hansen RJ (2010) Properties of a general PK/PD model of antibody-ligand interactions for therapeutic antibodies that bind to soluble endogenous targets. *MAbs* **2:** 576-588.

Deng R, Jin F, Prabhu S, and Iyer S (2012) Monoclonal antibodies: what are the pharmacokinetic and pharmacodynamic considerations for drug development? *Expert Opin Drug Metab Toxicol* **8:** 141-160.

DeVay RM, Shelton DL, and Liang H (2013) Characterization of proprotein convertase subtilisin/kexin type 9 (PCSK9) trafficking reveals a novel lysosomal targeting mechanism via amyloid precursor-like protein 2 (APLP2). *Journal of Biological Chemistry* **288:** 10805-10818.

Finch DK, Sleeman MA, Moisan J, Ferraro F, Botterell S, Campbell J, Cochrane D, Cruwys S, England E, Lane S, Rendall E, Sinha M, Walker C, Rees G, Bowen MA, Schneider A, Liang M, Faggioni R, Fung M, Mallinder PR, Wilkinson T, Kolbeck R, Vaughan T, and Lowe DC (2011) Whole-molecule antibody engineering: generation of a high-affinity anti-IL-6 antibody with extended pharmacokinetics. *J Mol Biol* **411:** 791-807.

Getz GS and Reardon CA (2012) Animal models of atherosclerosis. *Arterioscler Thromb Vasc Biol* **32:** 1104-1115.

Grundy SM, Cleeman JI, Merz CN, Brewer HB, Jr., Clark LT, Hunninghake DB, Pasternak RC, Smith SC, Jr., Stone NJ, National Heart L, Blood I, American College of Cardiology F, and American Heart A (2004) Implications of recent clinical trials for the National Cholesterol Education Program Adult Treatment Panel III guidelines. *Circulation* **110:** 227-239.

Hinton PR, Johlfs MG, Xiong JM, Hanestad K, Ong KC, Bullock C, Keller S, Tang MT, Tso JY, Vasquez M, and Tsurushita N (2004) Engineered human IgG antibodies with longer serum half-lives in primates. *J Biol Chem* **279:** 6213-6216.

Hooper AJ and Burnett JR (2013) Anti-PCSK9 therapies for the treatment of hypercholesterolemia. *Expert Opin Biol Ther* **13:** 429-435.

Hopkins CR and Trowbridge IS (1983) Internalization and processing of transferrin and the transferrin receptor in human carcinoma A431 cells. *J Cell Biol* **97:** 508-521.

Horton JD, Cohen JC, and Hobbs HH (2007) Molecular biology of PCSK9: its role in LDL metabolism. *Trends Biochem Sci* **32:** 71-77.

Igawa T, Ishii S, Tachibana T, Maeda A, Higuchi Y, Shimaoka S, Moriyama C, Watanabe T, Takubo R, Doi Y, Wakabayashi T, Hayasaka A, Kadono S, Miyazaki T, Haraya K, Sekimori Y, Kojima T, Nabuchi Y, Aso Y, Kawabe Y, and Hattori K (2010) Antibody recycling by engineered pH-dependent antigen binding improves the duration of antigen neutralization. *Nat Biotechnol* **28:** 1203-1207.

Kuo TT and Aveson VG (2011) Neonatal Fc receptor and IgG-based therapeutics. *MAbs* **3:** 422-430.

Lagace TA, Curtis DE, Garuti R, McNutt MC, Park SW, Prather HB, Anderson NN, Ho YK, Hammer RE, and Horton JD (2006) Secreted PCSK9 decreases the number of LDL receptors in hepatocytes and in livers of parabiotic mice. *J Clin Invest* **116:** 2995-3005.

Levy G (1994) Pharmacologic target-mediated drug disposition. *Clin Pharmacol Ther* **56:** 248-252.

Liang H, Chaparro-Riggers J, Strop P, Geng T, Sutton JE, Tsai D, Bai L, Abdiche Y, Dilley J, Yu J, Wu S, Chin SM, Lee NA, Rossi A, Lin JC, Rajpal A, Pons J, and Shelton DL (2012) Proprotein convertase substilisin/kexin type 9 antagonism reduces low-density lipoprotein cholesterol in statin-treated hypercholesterolemic nonhuman primates. *J Pharmacol Exp Ther* **340:** 228-236.

National Research Council (2011) Guide for the Care and Use of Laboratory Animals, 8th ed. The National Acdemies Press, Washington, DC.

Ni YG, Di Marco S, Condra JH, Peterson LB, Wang W, Wang F, Pandit S, Hammond HA, Rosa R, Cummings RT, Wood DD, Liu X, Bottomley MJ, Shen X, Cubbon RM, Wang SP, Johns DG, Volpari C, Hamuro L, Chin J, Huang L, Zhao JZ, Vitelli S, Haytko P, Wisniewski D, Mitnaul LJ, Sparrow CP, Hubbard B, Carfi A, and Sitlani A (2011) A PCSK9-binding antibody that

structurally mimics the EGF(A) domain of LDL-receptor reduces LDL cholesterol in vivo. *J Lipid Res* **52:** 78-86.

Ober RJ, Martinez C, Vaccaro C, Zhou J, and Ward ES (2004) Visualizing the site and dynamics of IgG salvage by the MHC class I-related receptor, FcRn. *J Immunol* **172:** 2021-2029.

Piper DE, Jackson S, Liu Q, Romanow WG, Shetterly S, Thibault ST, Shan B, and Walker NP (2007) The crystal structure of PCSK9: a regulator of plasma LDL-cholesterol. *Structure* **15:** 545-552.

Pokala N and Handel TM (2005) Energy functions for protein design: adjustment with protein-protein complex affinities, models for the unfolded state, and negative design of solubility and specificity. *Journal of Molecular Biology* **347:** 203-227.

Robbie GJ, Criste R, Dall'acqua WF, Jensen K, Patel NK, Losonsky GA, and Griffin MP (2013) A novel investigational Fc-modified humanized monoclonal antibody, motavizumab-YTE, has an extended half-life in healthy adults. *Antimicrob Agents Chemother* **57:** 6147-6153.

Robinson JG, Nedergaard BS, Rogers WJ, Fialkow J, Neutel JM, Ramstad D, Somaratne R, Legg JC, Nelson P, Scott R, Wasserman SM, Weiss R, and Investigators L- (2014) Effect of evolocumab or ezetimibe added to moderate- or high-intensity statin therapy on LDL-C lowering in patients with hypercholesterolemia: the LAPLACE-2 randomized clinical trial. *JAMA* **311:** 1870-1882.

Roopenian DC and Akilesh S (2007) FcRn: the neonatal Fc receptor comes of age. *Nat Rev Immunol* **7:** 715-725.

Seidah NG, Benjannet S, Wickham L, Marcinkiewicz J, Jasmin SB, Stifani S, Basak A, Prat A, and Chretien M (2003) The secretory proprotein convertase neural apoptosis-regulated convertase 1 (NARC-1): liver regeneration and neuronal differentiation. *Proc Natl Acad Sci U S A* **100:** 928-933.

Stancu C and Sima A (2001) Statins: mechanism of action and effects. *J Cell Mol Med* **5:** 378-387.

Stein EA and Raal F (2014) Reduction of low-density lipoprotein cholesterol by monoclonal antibody inhibition of PCSK9. *Annu Rev Med* **65:** 417-431.

Stroes E, Colquhoun D, Sullivan D, Civeira F, Rosenson RS, Watts GF, Bruckert E, Cho L, Dent R, Knusel B, Xue A, Scott R, Wasserman SM, Rocco M, and Investigators G- (2014) Anti-PCSK9 Antibody Effectively Lowers Cholesterol in Patients With Statin Intolerance: The GAUSS-2 Randomized, Placebo-Controlled Phase 3 Clinical Trial of Evolocumab. *J Am Coll Cardiol* **63:** 2541-2548.

Tabrizi M, Bornstein GG, and Suria H (2010) Biodistribution mechanisms of therapeutic monoclonal antibodies in health and disease. *AAPS J* **12:** 33-43.

Tavori H, Fan D, Blakemore JL, Yancey PG, Ding L, Linton MF, and Fazio S (2013) Serum proprotein convertase subtilisin/kexin type 9 and cell surface low-density lipoprotein receptor: evidence for a reciprocal regulation. *Circulation* **127:** 2403-2413.

Wang W, Lu P, Fang Y, Hamuro L, Pittman T, Carr B, Hochman J, and Prueksaritanont T (2011) Monoclonal antibodies with identical Fc sequences can bind to FcRn differentially with pharmacokinetic consequences. *Drug Metab Dispos* **39:** 1469-1477.

Zalevsky J, Chamberlain AK, Horton HM, Karki S, Leung IW, Sproule TJ, Lazar GA, Roopenian DC, and Desjarlais JR (2010) Enhanced antibody half-life improves in vivo activity. *Nat Biotechnol* **28:** 157-159.

Figure Legends.

Figure 1. (A) Mean (±SD) intravenous pharmacokinetic profiles of mAb1 and IgG2 Control in C57Bl/6 (WT) and PCSK9$^{-/-}$ (KO) mice at doses of 3 mg/kg. (B) Mean (±SD) intravenous pharmacokinetic profiles of mAb1 following administration alone (closed circles) or as a 1:2 bivalent complex (open circles) with human PCSK9 at molar equivalent doses of mAb1.

Figure 2. mAb1, mAb2, mAb3, mAb4 and IgG2 Control pharmacokinetics, total serum PCSK9 concentrations, and LDL-C pharmacodynamics following subcutaneous administration of a 0.5 mg/kg dose to cynomolgus monkeys (n=5/group). (A) Mean (±SD) pharmacokinetic profiles; (B) Mean (±SEM) PCSK9 concentrations; (C) Mean (±SEM) LDL-C responses. Asterisks indicate the last time point at which LDL-C differed from pre-dose baseline in each group ($p<0.05$).

Figure 3. mAb1, mAb2, and respective YTE and LS Fc-variant pharmacokinetics and LDL-C pharmacodynamics following intravenous administration of a 1 (mAb2 and variants) or 3 (mAb1 and variants) mg/kg dose to cynomolgus monkeys (n=4/group). (A) Mean (±SD) pharmacokinetic profiles; (B) Mean (±SEM) LDL-C responses. PD sampling for mAb1 and its variants was discontinued on day 56. Asterisks indicate time points at which Fc-variant mAb2 LDL-C differed from native mAb2 ($p<0.05$).

Figure 4. mAb2, mAb3, and respective 8 and 119 Fc loop-insertion variant pharmacokinetics and LDL-C pharmacodynamics following intravenous administration of a 1 mg/kg dose to cynomolgus monkeys (n=4/group). (A) Mean (±SD) pharmacokinetic profiles; (B) Mean (±SEM) LDL-C responses. Asterisks indicate time points at which Fc-variant mAb3 LDL-C differed from native mAb3 ($p<0.05$). No statistical difference was noted for Fc-variant mAb2 LDL-C compared to native mAb2 throughout the duration of the study.

JPET Fast Forward. Published on February 4, 2015 as DOI: 10.1124/jpet.114.221242
This article has not been copyedited and formatted. The final version may differ from this version.

Table 1. Pharmacokinetics of mAb1 and IgG2 Control in C57Bl/6 (WT) and PCSK9$^{-/-}$ (KO) mice following intravenous administration.

Mouse Strain	Test Article	Dose (mg/kg)	AUC_{inf} (μg·h/mL)	AUC_{last} (μg·h/mL)	CL (mL/h/kg)	V_{ss} (mL/kg)	$t_{1/2,z}$ (h)
WT	mAb1	3	5700	5700	0.526	53.4	150
	IgG2 Control	3	21800	19700	0.138	78.9	390
KO	mAb1	3	21400	18300	0.140	92.1	580
	IgG2 Control	3	23100	20900	0.130	74.9	430
WT	mAb1	10	36400	36600	0.275	41.7	82
	mAb1:PCSK9	20*	3350	3340	2.99	151	64

*Dose level refers to mAb1:PCSK9 complex prepared at a 1:2 stoichiometric ratio. The molecular weight ratio of mAb1:PCSK9 is ~2:1, therefore the mAb1 equivalent dose was 10 mg/kg.

JPET Fast Forward. Published on February 4, 2015 as DOI: 10.1124/jpet.114.221242
This article has not been copyedited and formatted. The final version may differ from this version.

Table 2. Kinetic binding constants for mAb1, mAb2, mAb3, and mAb4 Fab fragment binding to recombinant cynomolgus monkey PCSK9 at pH 7.4 and 5.5, 25° C.

Antibody Fab	pH	k_a ($\times 10^5$ $M^{-1}s^{-1}$)	k_d ($\times 10^{-4}$ s^{-1})	$t_{1/2,dis}$ † (s)	$k_{d,5.5}$ / $k_{d,7.4}$	K_D (nM)	$K_{D,5.5}$ / $K_{D,7.4}$
mAb1	7.4	23.5 (0.009)	0.137 (0.0003)	51000		0.00596 (0.000002)	
	5.5	23.5 (0.02)	0.243 (0.0005)	28000	1.8	0.0102 (0.000008)	1.7
mAb2	7.4	2.47 (0.005)	11.2 (0.05)	620		4.55 (0.02)	
	5.5	0.991 (0.007)	670 (5)	10	60	676 (5)	150
mAb3	7.4	5.87 (0.004)	0.975 (0.0006)	7100		0.166 (0.0001)	
	5.5	1.64 (0.004)	88.7 (0.1)	78	91	54.2 (0.1)	330
mAb4	7.4	7.66 (0.01)	7.50 (0.04)	920		0.979 (0.004)	
	5.5	1.86 (0.006)	542 (4)	13	72	292 (9)	300

† $t_{1/2,dis}$=complex dissociation half-life=Ln2/k_d. The standard deviation to the 1:1 binding model fit is indicated in parentheses.

Table 3. Summary of mean anti-PCSK9 antibody pharmacokinetics (±SD) and LDL-C pharmacodynamics (±SEM) in monkeys.

			Antibody Pharmacokinetics							LDL-C Pharmacodynamics		
Antibody	Dose* (mg/kg)	N	AUC_{inf} (μg·h/mL)	AUC_{last} (μg·h/mL)	CL (mL/h/kg)	V_{ss} (mL/kg)	CL/F (mL/h/kg)	C_{max} (μg/mL)	$t_{1/2,z}$ (h)	E_{max} (mg/dL)	ECA (mg·d/dL)	Duration (d)
mAb1	0.5	5	370±52	364±53	--	--	1.37±0.17	4.84±0.62	49±18	41±5	422±97	6
	3	3	4410±300	4400±300	0.683±0.047	44.1±4.6	--	--	42±4	44±5	531±109	10
mAb1_YTE	3	4	5460±2590	5460±2590	0.650±0.307	53.1±9.3	--	--	52±9	52±7	608±178	10
mAb1_LS	3	4	4430±910	4420±450	0.684±0.075	49.3±4.8	--	--	43±4	47±6	508±112	10
mAb2	0.5	5	4180±700	3810±490	--	--	0.123±0.021	9.27±0.27	340±70	37±7	1230±280	51
	1[†]	4	6050±450	5960±830	0.168±0.026	56.3±3.7	--	--	270±70	40±5	1280±250	35
	1[‡]	4	4650±850	4540±790	0.222±0.049	81.1±14.4	--	--	250±140	34±6	1100±280	36
mAb2_YTE	1	4	11000±1800	10100±1400	0.0931±0.0164	61.1±6.6	--	--	470±110	38±5	1490±390	42
mAb2_LS	1	4	9200±2560	8430±2130	0.118±0.044	67.7±15.2	--	--	420±230	44±4	1970±480	56
mAb2_8	1	4	7030±1360	6500±1070	0.147±0.034	75.8±18.8	--	--	430±230	36±4	1330±290	43
mAb2_119	1	4	4950±1530	4110±1630	0.217±0.068	59.4±13.8	--	--	200±130	40±7	1450±450	43
mAb3	0.5	5	1170±120	1160±120	--	--	0.432±0.043	6.64±0.68	150±40	47±5	925±128	18
	1	4	1590±190	1570±170	0.634±0.071	72.9±17.2	--	--	150±80	41±5	470±50	11
mAb3_8	1	4	2370±150	2360±150	0.422±0.026	61.2±9.5	--	--	140±60	38±6	718±226	18
mAb3_119	1	4	2700±510	2660±520	0.381±0.075	54.6±5.3	--	--	120±40	37±6	370±63	18
mAb4	0.5	5	2110±500	2020±490	--	--	0.249±0.067	6.09±0.71	250±140	42±5	1320±240	39
IgG2 Control	0.5	5	4030±790	3390±500	--	--	0.128±0.028	6.92±0.97	460±90	--	--	--

*Doses of 0.5 mg/kg were administered subcutaneously, and doses of 1 or 3 mg/kg were administered intravenously. [†]Data from Study 2. [‡]Data from Study 3, see Methods.

JPET Fast Forward. Published on February 4, 2015 as DOI: 10.1124/jpet.114.221242
This article has not been copyedited and formatted. The final version may differ from this version.

Table 4. Cynomolgus Monkey FcRn Binding EC_{50} Summary at pH 5.5.

Antibody	EC_{50} (nM)	95% Confidence Interval (nM)	Native EC_{50} / Variant EC_{50}
mAb1	105	86-130	--
mAb1_YTE	6.48	5.2-8.1	16
mAb1_LS	16.1	15-18	7
mAb2[†]	130	105-160	--
mAb2_YTE	11.7	11-13	11
mAb2_LS	17.8	16-20	7
mAb2[‡]	209	120-370	--
mAb2_8	3.09	2.7-3.6	68
mAb2_119	4.44	3.2-6.1	47
mAb3	125	100-150	--
mAb3_8	3.59	2.5-5.3	35
mAb3_119	3.62	3.1-4.2	35
mAb4	83.7	67-100	--
IgG2 Control	150	110-210	--

[†]Data from same experiment as YTE and LS variants.
[‡]Data from same experiment as 8 and 119 loop-insertion variants.

Figure 1

JPET Fast Forward. Published on February 4, 2015 as DOI: 10.1124/jpet.114.221242
This article has not been copyedited and formatted. The final version may differ from this version.

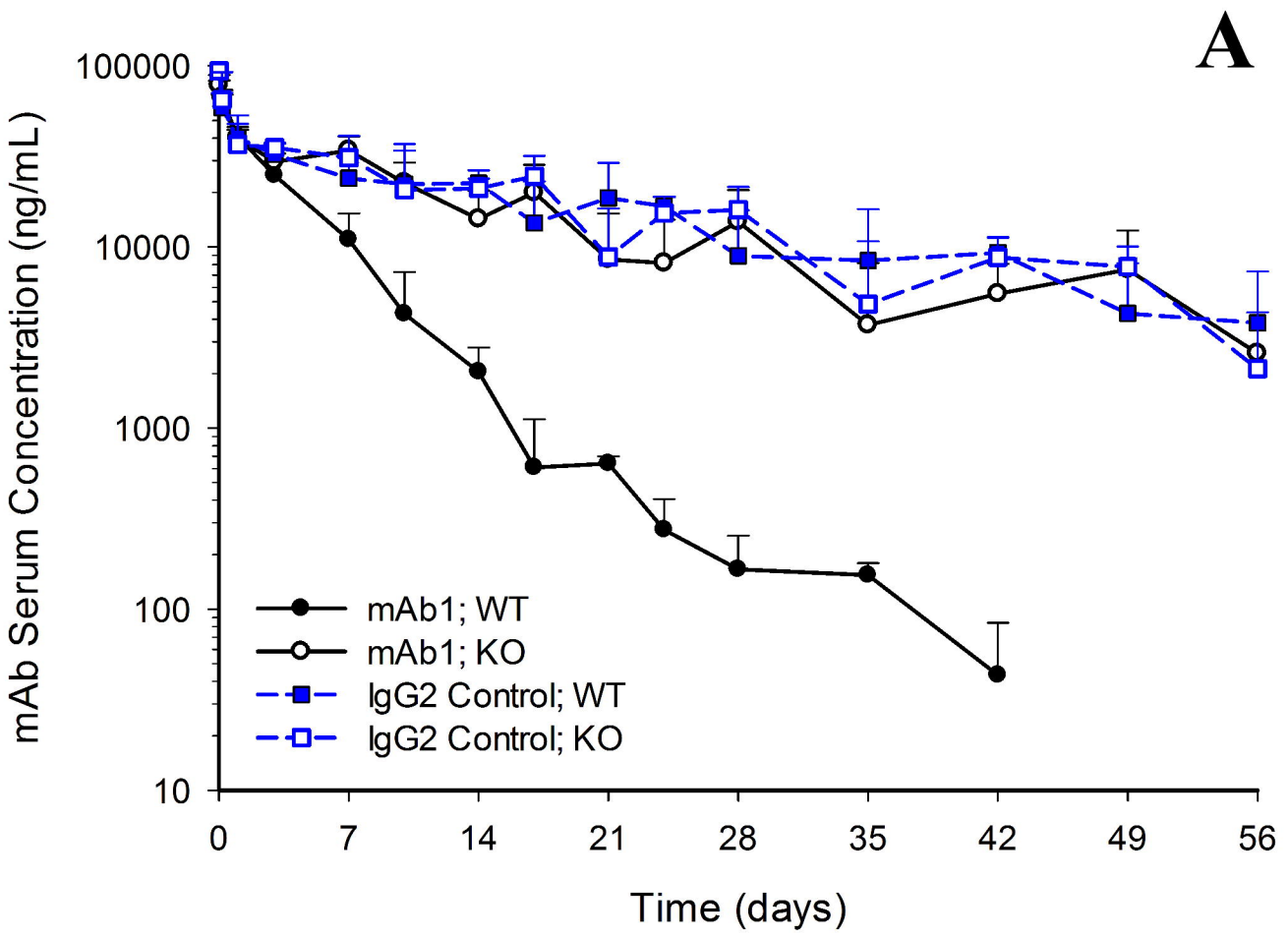

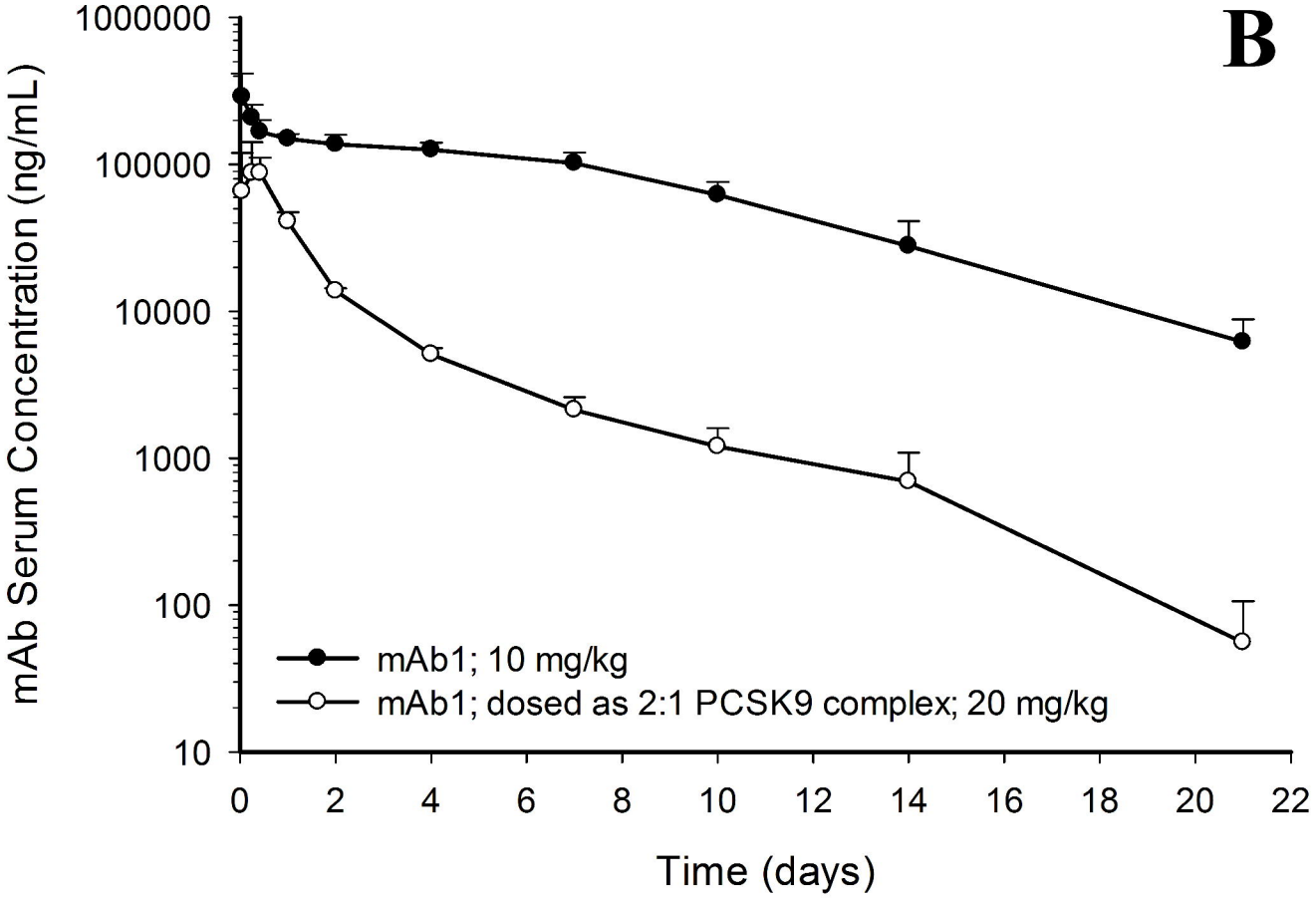

Figure 2

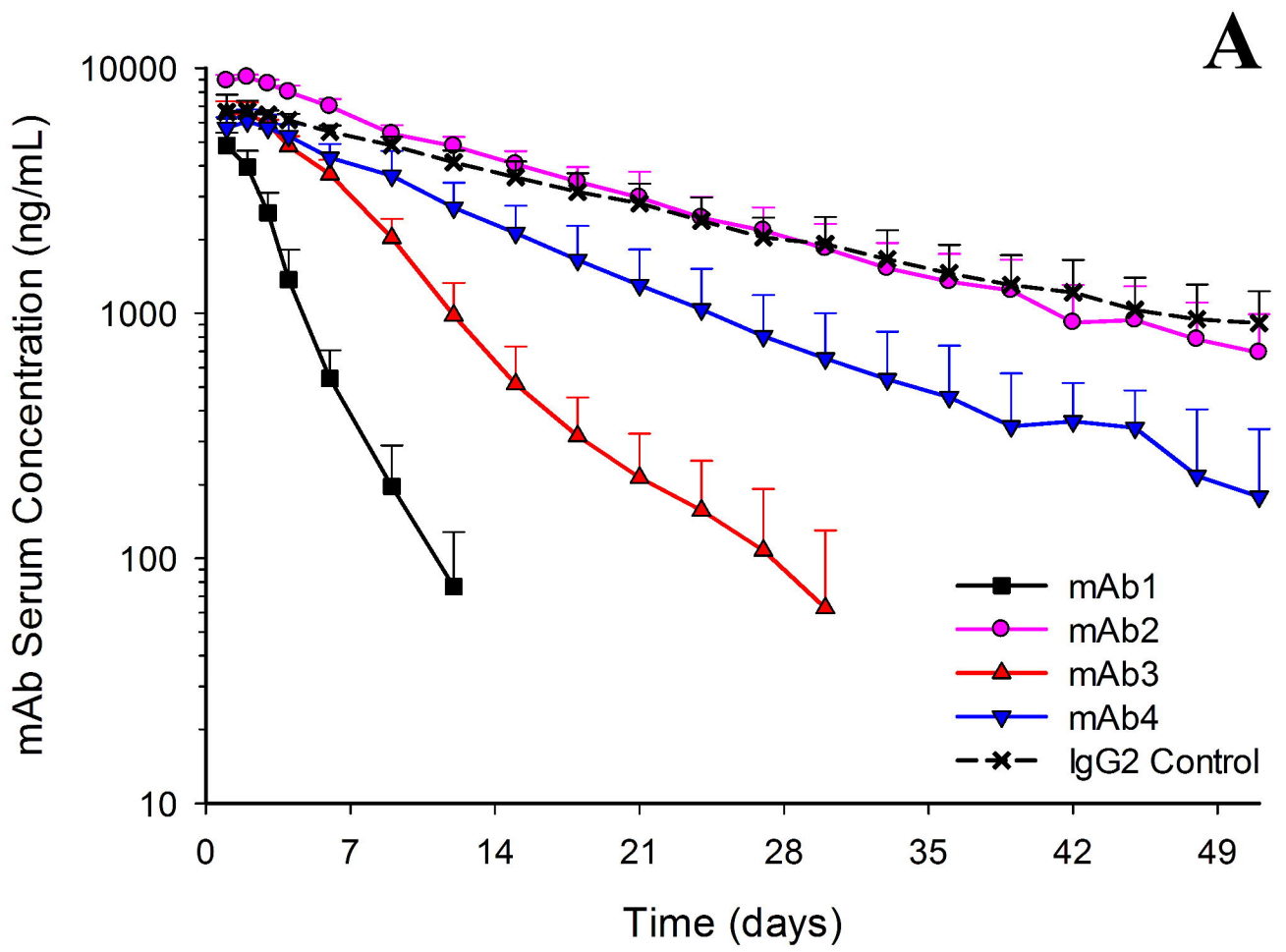

JPET Fast Forward. Published on February 4, 2015 as DOI: 10.1124/jpet.114.221242
This article has not been copyedited and formatted. The final version may differ from this version.

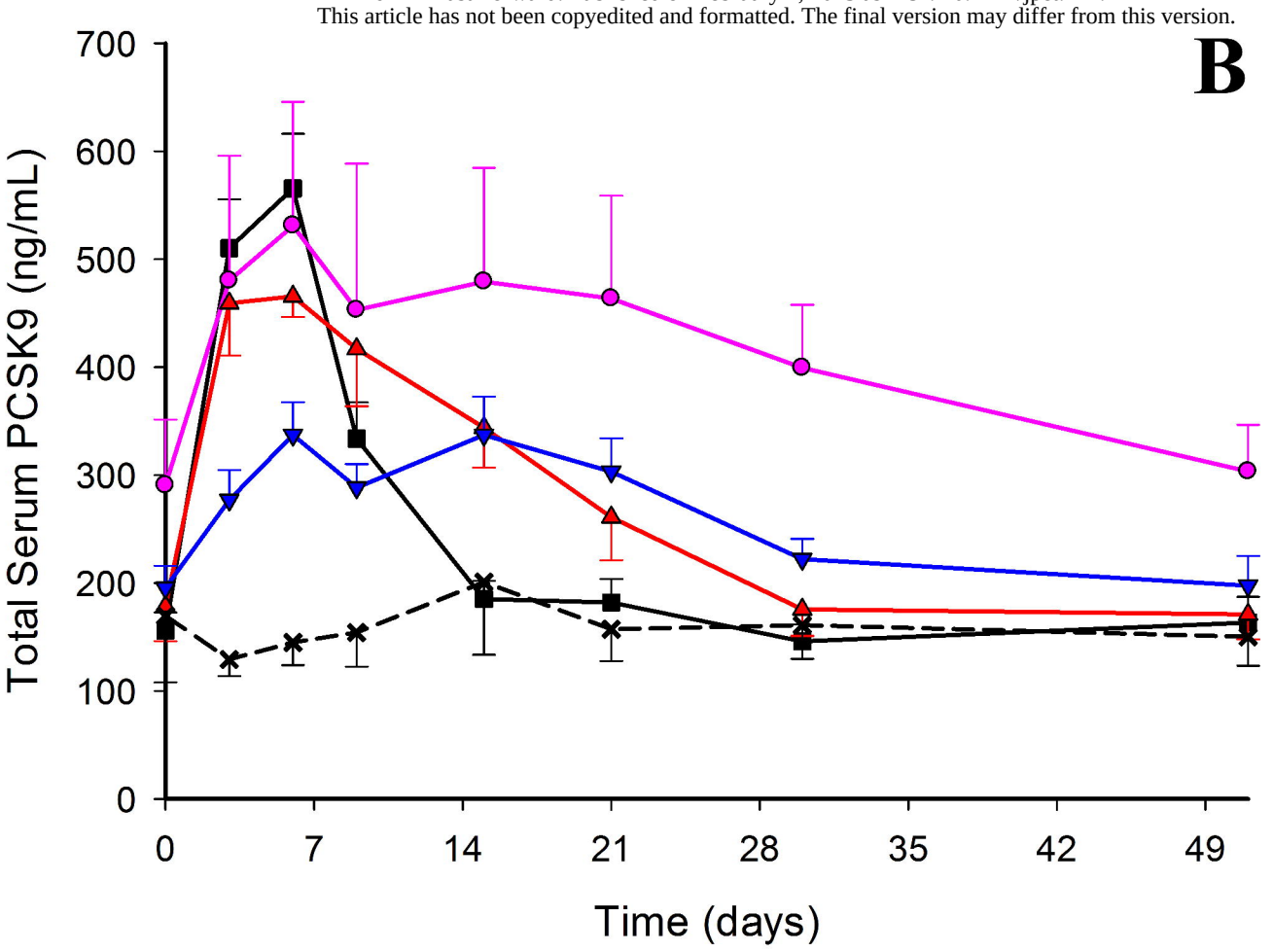

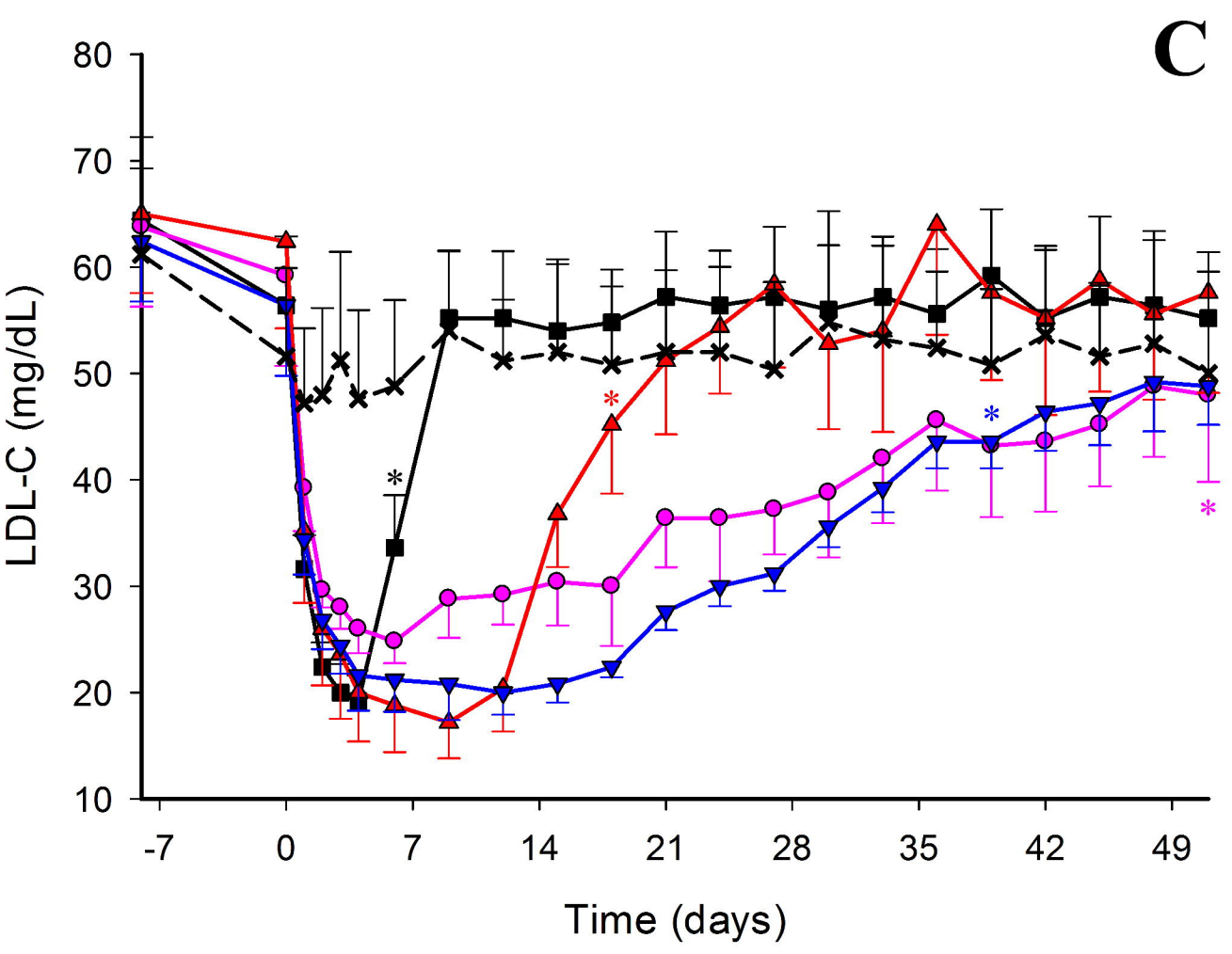

Figure 3

JPET Fast Forward. Published on February 4, 2015 as DOI: 10.1124/jpet.114.221242
This article has not been copyedited and formatted. The final version may differ from this version.

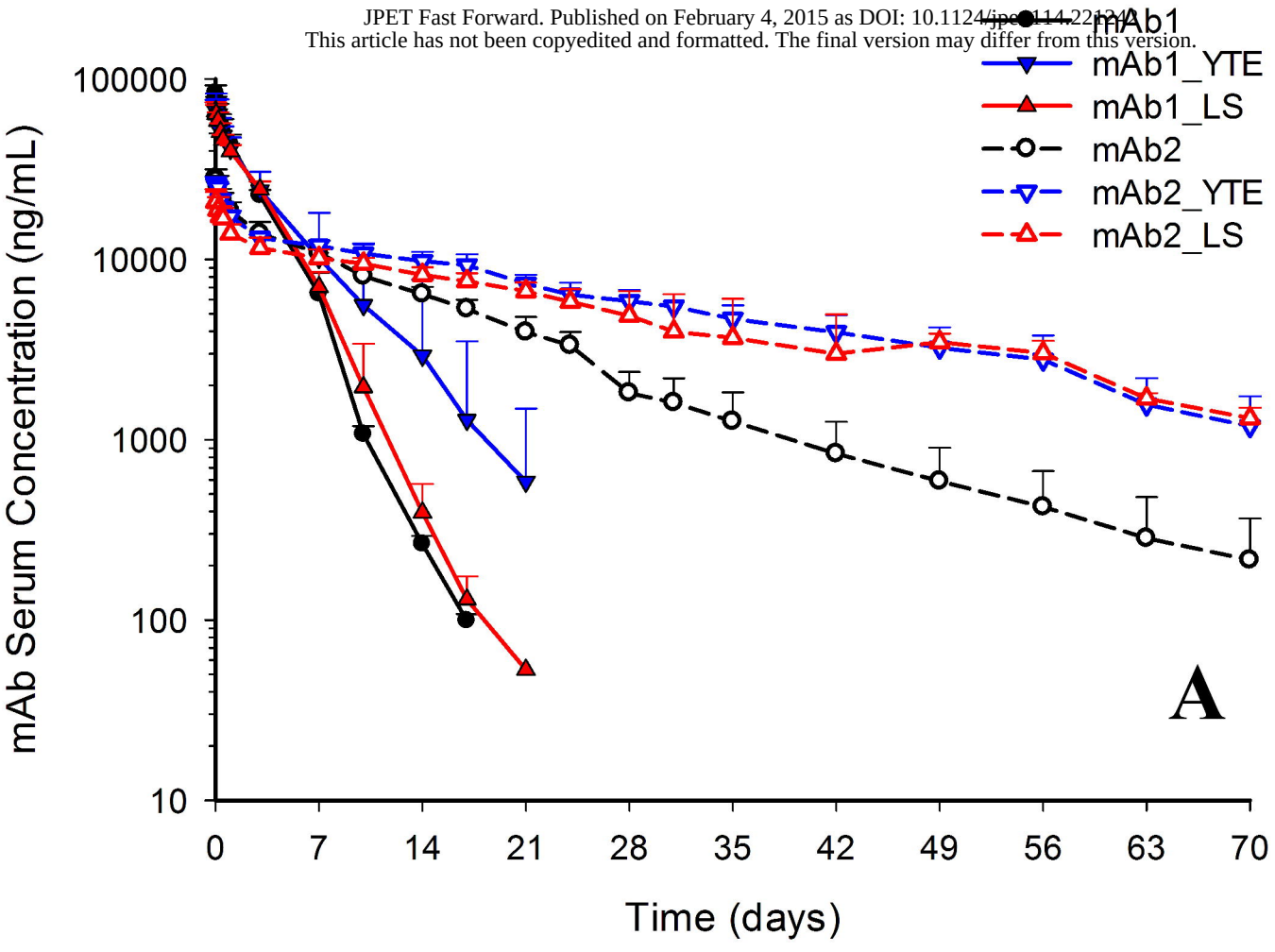

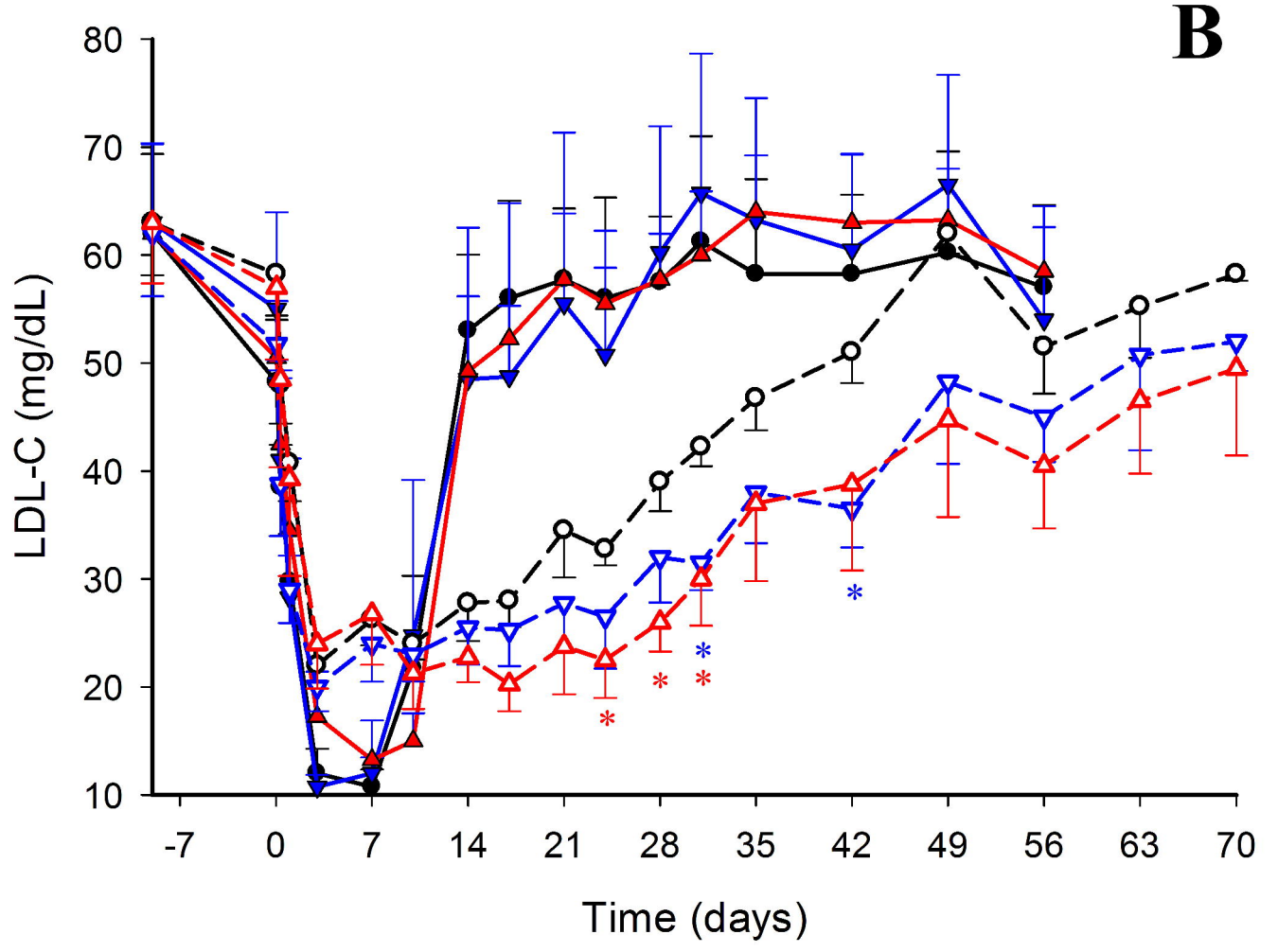

Figure 4

JPET Fast Forward. Published on February 4, 2015 as DOI: 10.1124/jpet.114.221242
This article has not been copyedited and formatted. The final version may differ from this version.